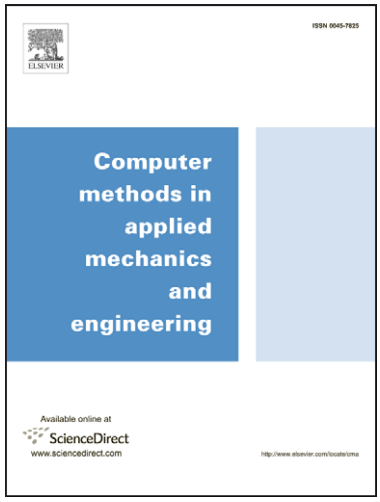

Steady-state nonlinear heat conduction in composite materials using the method of fundamental solutions

A. Karageorghis, D. Lesnic

PII: S0045-7825(08)00073-X
DOI: 10.1016/j.cma.2008.02.011
Reference: CMA 8591

To appear in: *Comput. Methods Appl. Mech. Engrg.*

Received Date: 4 May 2007
Revised Date: 14 January 2008
Accepted Date: 15 February 2008

Please cite this article as: A. Karageorghis, D. Lesnic, Steady-state nonlinear heat conduction in composite materials using the method of fundamental solutions, *Comput. Methods Appl. Mech. Engrg.* (2008), doi: 10.1016/j.cma.2008.02.011

STEADY-STATE NONLINEAR HEAT CONDUCTION IN COMPOSITE MATERIALS USING THE METHOD OF FUNDAMENTAL SOLUTIONS

A. KARAGEORGHIS AND D. LESNIC

Abstract. The steady-state heat conduction in composite (layered) heat conductors with temperature dependent thermal conductivity and mixed boundary conditions involving convection and radiation is investigated using the method of fundamental solutions with domain decomposition. The locations of the singularities outside the solution domain are optimally determined using a nonlinear least-squares procedure. Numerical results for nonlinear bimaterials are presented and discussed.

1. Introduction

In many heat transfer problems the assumption of constant thermal conductivity, i.e. that the heat conductors are homogeneous within the whole temperature variation interval, may lead to unacceptable errors in high-temperature environments or if large temperature differences are present, see [31]. In the steady-state situation, the nonlinearity associated with the temperature dependence of the thermal conductivity can be removed by employing the Kirchhoff transformation, which replaces the original nonlinear partial differential equation in divergence form by the Laplace equation in the transformed space, see [11]. Boundary conditions of the Dirichlet (first kind) or Neumann (second kind) types pose no problem for the transformation, but the Robin convective (third kind) boundary conditions become non-linear. Although this non-linearity is not strong, convergence problems may arise if radiative heat transfer (fourth kind) boundary conditions are also present, see [12]. Since all the non-linearities are transferred to the boundary conditions, the Kirchhoff transformation approach is very well-suited for applying the boundary element method (BEM), [7, 20], or, more recently, the method of fundamental solutions (MFS) [22, 23]. In the same manner these techniques can be extended to composite bodies through the subregion technique. In it, each region is dealt with separately and then the whole body is linked together by applying compatibility and equilibrium conditions along the interfaces between subregions.

Two-dimensional boundary value problems of heat conduction in nonlinear composite materials have been the subject of several studies using the BEM, [2, 6, 8]. However, the implementation of the BEM becomes quite tedious, especially in three-dimensional irregular domains. Moreover, the evaluation of the gradient of the temperature solution on the boundary requires the use of finite differences or the evaluation of hypersingular integrals. In order to alleviate some of these difficulties, we propose the use of the MFS. The merits and drawbacks of the MFS over the BEM for solving elliptic boundary value problems are thoroughly discussed in [10, 13, 14, 19, 25, 32]. Recently, the MFS has been made applicable to inhomogeneous elliptic equations [1] and inverse problems [33].

Prior to this study, the MFS was used for the solution of problems of heat conduction in linear layered materials with linear boundary conditions [3]. It is the purpose of this paper to extend this analysis to nonlinear materials with nonlinear boundary conditions.

Date: January 14, 2008.

2000 *Mathematics Subject Classification.* Primary 65N35; Secondary 65N38, 65H10.

Key words and phrases. nonlinear heat conduction, composite materials, method of fundamental solutions.

The mathematical formulation of the problem is given in Section 2. The MFS and its implementation are described in Section 3. Numerical results are presented in Section 4 and in Section 5 some conclusions and ideas for future applications are given.

2. Mathematical formulation

Consider a bounded domain $\Omega \subset \mathbb{R}^d$, $d \geq 2$, with piecewise smooth boundary $\partial\Omega$, formed from two (or more) subregions Ω_1 and Ω_2 separated by the interfacial surface $\Gamma_{12} = \partial\Omega_1 \cap \partial\Omega_2$. The material of subregion Ω_1 has a temperature dependent thermal conductivity $k_1 > 0$ and material of subregion Ω_2 has a different thermal conductivity $k_2 > 0$. The governing steady-state heat conduction equations are

$$\nabla \cdot (k_i(T_i)\, \nabla T_i) = 0, \quad \text{in} \quad \Omega_i, \quad i = 1, 2, \tag{2.1}$$

where T_i is the temperature solution in domain Ω_i, $i = 1, 2$, and, for the sake of simplicity, we have assumed that there is no heat generation within Ω. The technique developed in this paper is valid for bodies Ω consisting of an arbitrary finite number of subregions.

Boundary conditions of the mixed type can be prescribed at the external surface $\partial\Omega$ of the composite body $\Omega = \Omega_1 \cup \Omega_2$ and they include (dropping for simplicity the region subscript $i = 1, 2$):

(i) Dirichlet boundary conditions (prescribed temperature f)

$$T = f, \quad \text{on} \quad S_1. \tag{2.2}$$

(ii) Neumann boundary conditions (prescribed heat flux g)

$$-k(T)\, \frac{\partial T}{\partial n} = g, \quad \text{on} \quad S_2, \tag{2.3}$$

where $\boldsymbol{n}$ is the outward normal to the boundary $\partial\Omega$.

(iii) Robin boundary conditions (prescribed heat transfer coefficient h)

$$-k(T)\, \frac{\partial T}{\partial n} = h\,(T - T_f), \quad \text{on} \quad S_3, \tag{2.4}$$

where T_f is the temperature of fluid exchanging heat with surface S_3.

(iv) Radiation condition (prescribed fourth-order power law)

$$-k(T)\, \frac{\partial T}{\partial n} = \sigma\, \varepsilon\, (T^4 - T_s^4), \quad \text{on } S_4, \tag{2.5}$$

where $\sigma = 5.67051 \times 10^{-8} W/(m^2 K^4)$ is the Stefan-Boltzman constant and ε is the radiation interchange factor (emissivity) between the irradiated boundary S_4 and the environment, having a temperature T_s.

In (2.2)-(2.5) the boundary portions S_j, $j = \overline{1,4}$, which cover the boundary $\partial\Omega$, i.e. $\partial\Omega = \cup_{j=1}^{4} S_j$, have no common parts, i.e. $S_i \cap S_j = \emptyset$, $i \neq j$. Also, in the above boundary conditions the nonlinearity occurs mainly due to the heat radiation (2.5), although the method of solution can also allow nonlinearities to occur from a temperature dependent heat transfer coefficient $h(T)$, or from a temperature dependent radiation interchange factor $\varepsilon(T)$.

In addition to the above boundary conditions (2.2)-(2.5), both imperfect and ideal contact conditions can occur at the interface Γ_{12}, namely

(v) Interface continuity

$$-k(T_1)\,\frac{\partial T_1}{\partial n^+} = k(T_2)\,\frac{\partial T_2}{\partial n^-}, \quad \text{on } \Gamma_{12}, \tag{2.6}$$

where $\boldsymbol{n}^+$ and $\boldsymbol{n}^-$ are the outward normals to the boundaries $\partial\Omega_1 \cap \Gamma_{12}$ and $\partial\Omega_2 \cap \Gamma_{12}$, respectively, i.e. since $\Gamma_{12} = \partial\Omega_1 \cap \partial\Omega_2$ we have $\boldsymbol{n}^+ = -\boldsymbol{n}^-$.

(vi) Ideal contact (interface temperature continuity)

$$T_1 = T_2, \quad \text{on } S_5, \tag{2.7}$$

and imperfect contact (interface temperature jump)

$$T_1 = T_2 - R\,k(T_1)\,\frac{\partial T_1}{\partial n^+}, \quad \text{on } S_6, \tag{2.8}$$

where R is the contact resistance. In (2.7) and (2.8) the interface portions S_5 and S_6 cover Γ_{12}, i.e. $S_5 \cup S_6 = \Gamma_{12}$, and have no common parts, i.e. $S_5 \cap S_6 = \emptyset$.

2.1. **Kirchhoff transformation.** The governing nonlinear partial differential equations (2.1) can be easily transformed into the Laplace equation by employing the Kirchhoff transformation defined as, see e.g. [11] or [27],

$$\Psi_i = \psi_i(T_i) := \int_0^{T_i} \frac{k_i(\xi)}{k_{0_i}}\,d\xi, \quad i = 1, 2, \tag{2.9}$$

where $k_i(T) = k_{0_i}(1 + m_i(T_i))$, k_{0_i} are positive constants and $m_i(T_i) > -1$ are known functions.
Since $k_i > 0$, the inverse transformation to (2.9) exists and is given by

$$T_i = \psi_i^{-1}(\Psi_i), \quad i = 1, 2. \tag{2.10}$$

Under (2.9), problem (2.1)-(2.8) transforms into the equivalent form

$$\nabla^2\Psi_i = 0, \quad \text{in } \Omega_i, \quad i = 1, 2, \tag{2.11}$$

subject to the boundary conditions (dropping for simplicity the subscript $i = 1, 2$)

$$\Psi = \psi(f), \quad \text{on } S_1, \tag{2.12}$$

$$-k_0\,\frac{\partial \Psi}{\partial n} = g, \quad \text{on } S_2, \tag{2.13}$$

$$-k_0\,\frac{\partial \Psi}{\partial n} = h\,[\psi^{-1}(\Psi) - T_f], \quad \text{on } S_3, \tag{2.14}$$

$$-k_0\,\frac{\partial \Psi}{\partial n} = \sigma\,\epsilon\,[\psi^{-1}(\Psi)^4 - T_s^4], \quad \text{on } S_4, \tag{2.15}$$

and the interface conditions

$$-k_{0_1}\,\frac{\partial \Psi_1}{\partial n^+} = k_{0_2}\,\frac{\partial \Psi_2}{\partial n^-}, \quad \text{on } \Gamma_{12}, \tag{2.16}$$

$$\psi_1^{-1}(\Psi_1) = \psi_2^{-1}(\Psi_2), \quad \text{on } S_5, \tag{2.17}$$

$$\psi_1^{-1}(\Psi_1) = \psi_2^{-1}(\Psi_2) - R\,k_{0_1}\,\frac{\partial \Psi_1}{\partial n^+}, \quad \text{on } S_6. \tag{2.18}$$

It can be seen that in the Kirchhoff space of the transform, the governing equation (2.11), the Dirichlet boundary condition (2.12), the Neumann boundary condition (2.13) and the flux continuity condition (2.16) are linear, whilst the convective boundary condition (2.14) and the interface temperature conditions (2.17) and (2.18) become nonlinear. The nonlinearity caused by the fourth power law radiation (2.5) is also present in the space of transform (2.15), and furthermore, the Kirchhoff transform is no longer continuous across the interface S_5, i.e. a jump in the transforms occurs there where $\Psi_1 \neq \Psi_2$.

The advantage of employing the Kirchhoff transformation (2.9) is that the MFS can now be applied for approximating the solution of the Laplace equation (2.11). This implies that all the advantages the MFS has over other methods, which are well-documented [14, 19], can be exploited. In particular, the fact that the MFS is a meshless boundary-type method renders the implementation of the method to problems in irregular domains and to three-dimensional problems straight-forward.

The solvability of problem (2.1)-(2.8), or equivalently the transformed problem (2.11)-(2.18) depends on the form, e.g. smoothness, monotonicity, of the input data Ω, $\partial\Omega$, Γ_{12}, k_i, f, g, T_f, T_s, h and ε and it may be established using classical boundary integral equation methods, see e.g. [17].

Once Ψ has been determined, the temperature solution T may be readily obtained from equation (2.10), via (2.9).

3. The method of fundamental solutions (MFS)

As the sources of nonlinearity are associated with the boundary conditions (2.14), (2.15), (2.17) and (2.18) only, the boundary value problem (2.11)-(2.18) for each subregion can, following [23], be converted into a minimization problem, or equivalently an algebraic system of nonlinear equations, using the MFS.

From [9, 26], the MFS approximations for the solutions Ψ_1 and Ψ_2 of the Laplace equation (2.11) have the form

$$\Psi^i_{\mathcal{N}}(\boldsymbol{c}^i, \boldsymbol{\xi}^i; \boldsymbol{x}) = \sum_{k=1}^{\mathcal{N}} c^i_k \, G_d(\boldsymbol{\xi}^i_k, \boldsymbol{x}), \quad \boldsymbol{x} \in \overline{\Omega}_i, \quad i = 1, 2, \tag{3.1}$$

where $\mathcal{N}$ is the number of unknown *singularities (sources)* $(\boldsymbol{\xi}^i_k)_{k=\overline{1,\mathcal{N}}} \notin \overline{\Omega}_i$, $(c^i_k)_{k=\overline{1,\mathcal{N}}}$ are unknown real coefficients and G_d is a fundamental solution for the Laplace equation, given by

$$G_d(\boldsymbol{\xi}, \boldsymbol{x}) = \begin{cases} \ln \mid \boldsymbol{\xi} - \boldsymbol{x} \mid, & d = 2, \\ \\ \dfrac{1}{\mid \boldsymbol{\xi} - \boldsymbol{x} \mid}, & d = 3. \end{cases} \tag{3.2}$$

The heat flux is obtained by differentiating (3.1) with respect to the outward normal $\boldsymbol{n}$.

In (3.1), the coordinates of the singularities may be either preassigned, or let free and determined as part of the solution [14]. Here, we adopt the former option, where the singularities are fixed, although their location is parametrized by a single unknown parameter, as described at the end of this section. Therefore, in equation (3.1) there are $2\mathcal{N}$ unknowns, namely, the coefficients $(c^i_k)_{k=\overline{1,\mathcal{N}}}$, $i = 1, 2$. These coefficients can be determined by collocating (imposing) the boundary and interface conditions (2.12)-(2.18) at $\mathcal{M}_{\partial\Omega}$ distinct points on the boundary $\partial\Omega_1 \backslash \Gamma_{12}$, $\mathcal{M}_{\partial\Omega}$ distinct points on the boundary $\partial\Omega_2 \backslash \Gamma_{12}$, and $\mathcal{M}_{\Gamma}$ distinct points on the interface Γ_{12}. We denote the boundary points on each of the four parts $(S_\ell)_{\ell=\overline{1,4}} \subset \partial\Omega$ in the following way:

(1) On $S_1 \cap \partial\Omega_i$ we take $(\boldsymbol{x}^i_j)_{j=\overline{1,\mathcal{M}_1}}$
(2) On $S_2 \cap \partial\Omega_i$ we take $(\boldsymbol{x}^i_j)_{j=\overline{\mathcal{M}_1+1,\mathcal{M}_1+\mathcal{M}_2}}$
(3) On $S_3 \cap \partial\Omega_i$ we take $(\boldsymbol{x}^i_j)_{j=\overline{\mathcal{M}_1+\mathcal{M}_2+1,\mathcal{M}_1+\mathcal{M}_2+\mathcal{M}_3}}$
(4) On $S_4 \cap \partial\Omega_i$ we take $(\boldsymbol{x}^i_j)_{j=\overline{\mathcal{M}_1+\mathcal{M}_2+\mathcal{M}_3+1,\mathcal{M}_1+\mathcal{M}_2+\mathcal{M}_3+\mathcal{M}_4}}$

On the interface Γ_{12} we take:

(5) On S_5 we take $(\boldsymbol{x}_j)_{j=\overline{1,\mathcal{M}_5}}$

and

(6) On S_6 we take $(\boldsymbol{x}_j)_{j=\overline{\mathcal{M}_5+1,\mathcal{M}_5+\mathcal{M}_6}}$

Clearly, here we have that $\mathcal{M}_{\partial\Omega} = \mathcal{M}_1 + \mathcal{M}_2 + \mathcal{M}_3 + \mathcal{M}_4$ and $\mathcal{M}_\Gamma = \mathcal{M}_5 + \mathcal{M}_6$.
We thus have a total number of $2\mathcal{N}$ unknowns and a total of $2\mathcal{M}_{\partial\Omega} + 2\mathcal{M}_\Gamma$ conditions to be satisfied.

Substituting (3.1) into (2.12)-(2.18), we minimize the nonlinear least-squares objective function

$$
\begin{aligned}
S(\boldsymbol{c}^1, \boldsymbol{c}^2) := \sum_{i=1}^{2} \Bigg\{ & \sum_{j=1}^{\mathcal{M}_1} \left[\Psi^i_{\mathcal{N}}(\boldsymbol{c}^i, \boldsymbol{\xi}^i; \boldsymbol{x}^i_j) - \psi_i(f(\boldsymbol{x}^i_j)) \right]^2 + \sum_{j=\mathcal{M}_1+1}^{\mathcal{M}_1+\mathcal{M}_2} \left[-k_{0_i} \frac{\partial \Psi^i_{\mathcal{N}}}{\partial n}(\boldsymbol{c}^i, \boldsymbol{\xi}^i; \boldsymbol{x}^i_j) - g(\boldsymbol{x}^i_j) \right]^2 \\
& + \sum_{j=\mathcal{M}_1+\mathcal{M}_2+1}^{\mathcal{M}_1+\mathcal{M}_2+\mathcal{M}_3} \left[-k_{0_i} \frac{\partial \Psi^i_{\mathcal{N}}}{\partial n}(\boldsymbol{c}^i, \boldsymbol{\xi}^i; \boldsymbol{x}^i_j) - h(\boldsymbol{x}^i_j) \left(\psi_i^{-1}(\Psi^i_{\mathcal{N}}(\boldsymbol{c}^i, \boldsymbol{\xi}^i; \boldsymbol{x}^i_j)) - T_f(\boldsymbol{x}^i_j)\right) \right]^2 \\
& + \sum_{j=\mathcal{M}_1+\mathcal{M}_2+\mathcal{M}_3+1}^{\mathcal{M}_{\partial\Omega}} \left[-k_{0_i} \frac{\partial \Psi^i_{\mathcal{N}}}{\partial n}(\boldsymbol{c}^i, \boldsymbol{\xi}^i; \boldsymbol{x}^i_j) - \sigma\, \varepsilon(\boldsymbol{x}^i_j) \left(\psi_i^{-1}(\Psi^i_{\mathcal{N}}(\boldsymbol{c}^i, \boldsymbol{\xi}^i; \boldsymbol{x}^i_j))^4 - T_s(\boldsymbol{x}^i_j)^4\right) \right]^2 \Bigg\} \\
& + \sum_{j=1}^{\mathcal{M}_5} \left[\psi_1^{-1}(\Psi^1_{\mathcal{N}}(\boldsymbol{c}^1, \boldsymbol{\xi}^1; \boldsymbol{x}_j)) - \psi_2^{-1}(\Psi^2_{\mathcal{N}}(\boldsymbol{c}^2, \boldsymbol{\xi}^2; \boldsymbol{x}_j)) \right]^2 \\
& + \sum_{j=\mathcal{M}_5+1}^{\mathcal{M}_\Gamma} \left[\psi_1^{-1}(\Psi^1_{\mathcal{N}}(\boldsymbol{c}^1, \boldsymbol{\xi}^1; \boldsymbol{x}_j)) - \psi_2^{-1}(\Psi^2_{\mathcal{N}}(\boldsymbol{c}^2, \boldsymbol{\xi}^2; \boldsymbol{x}_j)) + R\, k_{0_1} \frac{\partial \Psi^1_{\mathcal{N}}(\boldsymbol{c}^1, \boldsymbol{\xi}^1; \boldsymbol{x}_j)}{\partial n^+} \right]^2 \\
& + \sum_{j=1}^{\mathcal{M}_\Gamma} \left[-k_{0_1} \frac{\partial \Psi^1_{\mathcal{N}}(\boldsymbol{c}^1, \boldsymbol{\xi}^1; \boldsymbol{x}_j)}{\partial n^+} - k_{0_2} \frac{\partial \Psi^2_{\mathcal{N}}(\boldsymbol{c}^2, \boldsymbol{\xi}^2; \boldsymbol{x}_j)}{\partial n^-} \right]^2 . \qquad (3.3)
\end{aligned}
$$

The minimization of (3.3) is carried out using the MINPACK [16], routines `lmdif` or `lmder` which minimize the sum of the squares of nonlinear functions. In `lmder` the Jacobian is provided by the user, whilst in `lmdif` the Jacobian is calculated internally by forward finite differences. In this work both subroutines were used and it was found that `lmder` converged faster than `lmdif`. A comparison of the performance of the two subroutines may be found in [23].
In our experience, in the application of the MFS, unless there is good reason not to, the boundary points and sources are located uniformly, or as uniformly as possible, on the boundary and pseudoboundary, respectively. The case when it is advisable not to distribute these uniformly is when the method is applied to problems with boundary singularities, in which case the concentration of boundary points and sources near the boundary singularities leads to improved results, see e.g. [21]. In general, however, one needs to be careful with a highly non-uniform distribution of the boundary points and sources, since such a distribution may add to the ill-conditioning of the resulting MFS system of equations.
In the application of the MFS to bimaterials, two pseudo-boundaries were taken as exterior similar deformations $\partial\Omega'_i$ of the boundaries of the original domains $\Omega_i \subset \Omega'_i$, $i = 1, 2$. A number of $\mathcal{N}$ singularities was placed on each pseudo-boundary. An important question in the implementation of the MFS is the positioning of these pseudo-boundaries. We addressed this point by extending the approach used in [30]. In particular, the pseudo-boundaries $\partial\Omega'_i$, $i = 1, 2$ were taken at a distance $\eta > 0$ from the boundaries $\partial\Omega_i$, $i = 1, 2$, respectively, see Figures 1, 7, 11 and 14. In order to determine the optimal value of η, the minimization problem was solved for various values of $\eta_\ell = \eta_0 + \ell\,(\delta\eta)$, $\ell = \overline{1, L}$. For each η_ℓ, the maximum error in the boundary conditions at a selected set of uniformly spaced points on the boundary $\partial\Omega$ (different from the boundary collocation points) was calculated. The optimal value of η was chosen the one for which the maximum error was minimized.

The MFS formulation described in this section may be viewed as a *domain decomposition technique*. Such approaches have been used, in conjunction with the MFS, in [3, 4, 5, 15].

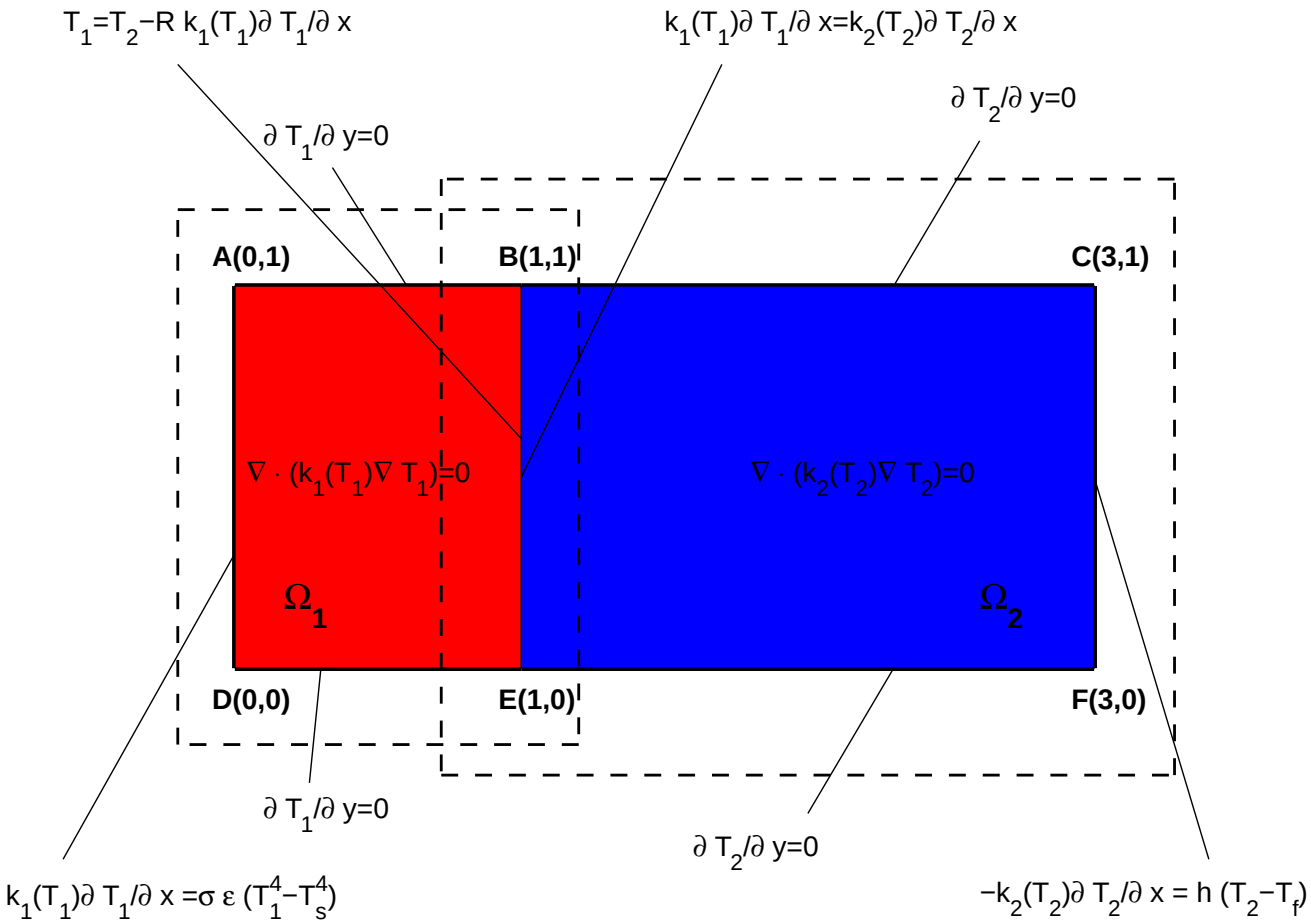

FIGURE 1. Geometry and boundary conditions for Example 1

4. Numerical results and discussion

In this section we present numerical results obtained from the application of the MFS described in the previous section.

4.1. **Example 1.** In order to validate the computational code and assess the accuracy of the numerical solution, we consider a problem investigated in [8] using the BEM, which possesses an analytical solution. The geometry and the boundary conditions are shown in Figure 1. The composite material $\Omega = \Omega_1 \cup \Omega_2$ is formed by layering the heat conductors $\Omega_1 = (0,1) \times (0,1)$ and $\Omega_2 = (1,3) \times (0,1)$. For many conductors, the thermal conductivity varies linearly with temperature, see [28], and we take

$$k_1(T_1) = k_{0_1}(1 + m_1(T_1)) = 1 + 0.1T_1,$$
$$k_2(T_2) = k_{0_2}(1 + m_2(T_2)) = 2(1 + 0.25T_2);\ W/(mK). \tag{4.1}$$

The sides ABC and DEF are insulated. On the front face AD the radiation condition with $\varepsilon = 0.3$ and $T_s = 800K$ is prescribed. The back face CF exchanges heat by convection with the heat transfer coefficient $h = 20W/(m^2K)$ and $T_f = 300K$. On the interface BE imperfect thermal contact with $R = 0.2m^2K/W$ is assumed. The mathematical

problem described above and in Figure 1 can be written as

$$\nabla \cdot ((1 + 0.1\,T_1)\ \nabla T_1) = 0, \quad \text{in } \Omega_1 = (0,1) \times (0,1), \tag{4.2}$$

$$\nabla \cdot (2\,(1 + 0.25\,T_2)\,\nabla T_2) = 0, \quad \text{in } \Omega_2 = (1,3) \times (0,1), \tag{4.3}$$

$$\frac{\partial T_1}{\partial y}(x,0) = \frac{\partial T_1}{\partial y}(x,1) = 0, \quad x \in (0,1), \tag{4.4}$$

$$\frac{\partial T_2}{\partial y}(x,0) = \frac{\partial T_2}{\partial y}(x,1) = 0, \quad x \in (1,3), \tag{4.5}$$

$$(1 + 0.1\,T_1(0,y))\ \frac{\partial T_1}{\partial x}(0,y) = 1.701153 \times 10^{-8}\ \left(T_1(0,y)^4 - 800^4\right), \quad y \in (0,1), \tag{4.6}$$

$$-\,2\ (1 + 0.25\,T_2(3,y))\ \frac{\partial T_2}{\partial x}(3,y) = 20\ (T_2(3,y) - 300), \quad y \in (0,1), \tag{4.7}$$

$$-\,(1 + 0.1\,T_1(1,y))\ \frac{\partial T_1}{\partial x}(1,y) = -2\ (1 + 0.25\,T_2(1,y))\ \frac{\partial T_2}{\partial x}(1,y), \quad y \in (0,1), \tag{4.8}$$

$$T_1(1,y) = T_2(1,y) - 0.2\ (1 + 0.1\,T_1(1,y))\ \frac{\partial T_1}{\partial x}(1,y), \quad y \in (0,1). \tag{4.9}$$

In order to obtain the analytical solution of this problem, one can observe from (4.4) and (4.5) that the temperature field is one-dimensional, varying only in the $x-$direction. Then (4.2), (4.3) and (4.8) yield

$$\begin{aligned} -\,(1 + 0.1\,T_1(x))\ T_1'(x) &= q = \text{constant}, \quad x \in [0,1], \\ -2\ (1 + 0.25\,T_2(x))\ T_2'(x) &= q = \text{constant}, \quad x \in [1,3], \end{aligned} \tag{4.10}$$

and from (4.6), (4.7) and (4.9) it follows that

$$-\,q = 1.701153 \times 10^{-8}(a^4 - 800^4), \quad q = 20(b - 300), \quad c = d + 0.2\,q, \tag{4.11}$$

where

$$a = T_1(0), \quad b = T_2(3), \quad c = T_1(1), \quad d = T_2(1).$$

Integrating (4.10) we obtain

$$-\,q = c - a + 0.05(c^2 - a^2), \quad -q = b - d + 0.125(b^2 - d^2). \tag{4.12}$$

Combining equations (4.11) and (4.12), we obtain a nonlinear system of five equations in the five unknowns q, a, b, c and d. We solved this system with Newton's method and obtained

$$q = 1638.3816070189441\,W/m^2,$$

$$\begin{aligned} T_1(0) = a &= 748.14643307239453\,K, \quad T_1(1) = c = 726.21897682687859\,K, \\ T_2(3) = b &= 381.91908035094718\,K, \quad T_2(1) = d = 398.54265542308980\,K. \end{aligned}$$

It is noteworthy that the results of Bialecki and Kuhn [8] are slightly different due to some mistakes in writing out the system of equations (4.11) and (4.12).

The analytical solution of the problem (4.2)-(4.9) is obtained by integrating (4.10) to yield

$$\begin{aligned} T_1(x) &= \frac{-1 + \sqrt{1 - 0.2\ (q\,x - a - 0.05\,a^2)}}{0.1}, \quad x \in [0,1], \\ T_2(x) &= \frac{-1 + \sqrt{1 - 0.25\ (q\,(x-1) - 2\,d - 0.25\,d^2)}}{0.25}, \quad x \in [1,3]. \end{aligned} \tag{4.13}$$

We next apply the Kirchhoff transformation and the MFS, as described in Sections 2.1 and 3, respectively, in order to compare the numerical solution with the analytical solution (4.13). Employing transformation (2.9) yields

$$\Psi_1 = \psi_1(T_1) = T_1 + 0.05\,T_1^2, \quad \Psi_2 = \psi_2(T_2) = T_2 + 0.125\,T_2^2. \tag{4.14}$$

The inverses of (4.14) are given by

$$T_1 = \psi_1^{-1}(\Psi_1) = \frac{-1+\sqrt{1+0.2\Psi_1}}{0.1}, \quad T_2 = \psi_2^{-1}(\Psi_2) = \frac{-1+\sqrt{1+0.5\Psi_2}}{0.25}, \tag{4.15}$$

where the negative roots are discarded since $k_1(T_1)$ and $k_2(T_2)$ have to be positive.
In the Kirchhoff transform space problem (4.2)-(4.9) becomes

$$\nabla^2\Psi_1(x,y) = 0, \quad (x,y) \in (0,1)\times(0,1), \tag{4.16}$$

$$\nabla^2\Psi_2(x,y) = 0, \quad (x,y) \in (1,3)\times(0,1), \tag{4.17}$$

$$\frac{\partial\Psi_1}{\partial y}(x,0) = \frac{\partial\Psi_1}{\partial y}(x,1) = 0, \quad x \in (0,1), \tag{4.18}$$

$$\frac{\partial\Psi_2}{\partial y}(x,0) = \frac{\partial\Psi_2}{\partial y}(x,1) = 0, \quad x \in (1,3), \tag{4.19}$$

$$\frac{\partial\Psi_1}{\partial x}(0,y) = 1.701153\times10^{-8}\left[\left(\frac{-1+\sqrt{1+0.2\,\Psi_1(0,y)}}{0.1}\right)^4 - 800^4\right], \quad y \in (0,1), \tag{4.20}$$

$$-2\,\frac{\partial\Psi_2}{\partial x}(3,y) = 20\left(\frac{-1+\sqrt{1+0.5\,\Psi_2(3,y)}}{0.25} - 300\right), \quad y \in (0,1), \tag{4.21}$$

$$-\frac{\partial\Psi_1}{\partial x}(1,y) = -2\,\frac{\partial\Psi_2}{\partial x}(1,y), \quad y \in (0,1), \tag{4.22}$$

$$\frac{-1+\sqrt{1+0.2\,\Psi_1(1,y)}}{0.1} = \frac{-1+\sqrt{1+0.5\,\Psi_2(1,y)}}{0.25} - 0.2\,\frac{\partial\Psi_1}{\partial x}(1,y), \quad y \in (0,1). \tag{4.23}$$

Remark that the linear Robin condition (4.7) has been transformed into the nonlinear Robin condition (4.21).

With the notation of Section 3, for problem (4.16)-(4.23), we have that $\mathcal{M}_1 = \mathcal{M}_5 = 0$ since no Dirichlet boundary conditions (2.2) or ideal contact interface temperature conditions (2.7) are present. Further, we chose $\mathcal{M}_2 = 2M$, $\mathcal{M}_3 = \mathcal{M}_4 = \mathcal{M}_\Gamma = M$, which yields a total of $8M$ boundary conditions. Thus, the nonlinear least-squares objective function (3.3) takes the form

$$\begin{aligned}
S(\boldsymbol{c}^1,\boldsymbol{c}^2) = &\sum_{i=1}^{2}\sum_{j=1}^{2M}\left[\frac{\partial\Psi^i_{\mathcal{N}}}{\partial y}(\boldsymbol{c}^i,\boldsymbol{\xi}^i;\boldsymbol{x}^i_j)\right]^2 \\
&+\sum_{j=2M+1}^{3M}\left[2\,\frac{\partial\Psi^2_{\mathcal{N}}}{\partial x}(\boldsymbol{c}^2,\boldsymbol{\xi}^2;\boldsymbol{x}^2_j) + 20\left(\frac{-1+\sqrt{1+0.5\,\Psi^2_{\mathcal{N}}(\boldsymbol{c}^2,\boldsymbol{\xi}^2;\boldsymbol{x}^2_j)}}{0.25} - 300\right)\right]^2 \\
&+\sum_{j=2M+1}^{3M}\left\{\frac{\partial\Psi^1_{\mathcal{N}}}{\partial x}(\boldsymbol{c}^1,\boldsymbol{\xi}^1;\boldsymbol{x}^1_j) - 1.701153\times10^{-8}\left[\left(\frac{-1+\sqrt{1+0.2\,\Psi^1_{\mathcal{N}}(\boldsymbol{c}^1,\boldsymbol{\xi}^1;\boldsymbol{x}^1_j)}}{0.1}\right)^4 - 800^4\right]\right\}^2 \\
&+\sum_{j=1}^{M}\left[\frac{-1+\sqrt{1+0.2\Psi^1_{\mathcal{N}}(\boldsymbol{c}^1,\boldsymbol{\xi}^1;\boldsymbol{x}_j)}}{0.1} - \frac{-1+\sqrt{1+0.5\,\Psi^2_{\mathcal{N}}(\boldsymbol{c}^2,\boldsymbol{\xi}^2;\boldsymbol{x}_j)}}{0.25} + 0.2\,\frac{\partial\Psi^1_{\mathcal{N}}}{\partial x}(\boldsymbol{c}^1,\boldsymbol{\xi}^1;\boldsymbol{x}_j)\right]^2 \\
&+\sum_{j=1}^{M}\left[-\frac{\partial\Psi^1_{\mathcal{N}}}{\partial x}(\boldsymbol{c}^1,\boldsymbol{\xi}^1;\boldsymbol{x}_j) + 2\frac{\partial\Psi^2_{\mathcal{N}}}{\partial x}(\boldsymbol{c}^2,\boldsymbol{\xi}^2;\boldsymbol{x}_j)\right]^2,
\end{aligned} \tag{4.24}$$

where the boundary collocation points are given by

$$\boldsymbol{x}_j^1 = \left(\frac{j}{M+1}, 0\right), \quad \boldsymbol{x}_{M+j}^1 = \left(\frac{j}{M+1}, 1\right), \quad \boldsymbol{x}_{2M+j}^1 = \left(0, \frac{j-1}{M-1}\right), \tag{4.25}$$

$$\boldsymbol{x}_j^2 = \left(1+\frac{2j}{M+1}, 0\right), \quad \boldsymbol{x}_{M+j}^2 = \left(1+\frac{2j}{M+1}, 1\right), \quad \boldsymbol{x}_{2M+j}^2 = \left(3, \frac{j-1}{M-1}\right), \tag{4.26}$$

$$\text{and} \qquad \boldsymbol{x}_j = \left(1, \frac{j-1}{M-1}\right), \qquad j = \overline{1, M}. \tag{4.27}$$

With respect to Figure 1, the source points $(\boldsymbol{\xi}_k^1)_{k=\overline{1,\mathcal{N}}}$ and $(\boldsymbol{\xi}_k^2)_{k=\overline{1,\mathcal{N}}}$ are located on pseudo-boundaries $\partial\Omega_1'$ and $\partial\Omega_2'$ which enclose and are similar to the domains Ω_1 and Ω_2, respectively, at a distance $\eta > 0$ from them. On each pseudo-boundary the $\mathcal{N}$ sources are distributed in a similar way to the distribution of the boundary points. In particular we take $\mathcal{N} = 4N$ and place N sources on each side of the rectangle $\partial\Omega_i'$, $i = 1, 2$, and thus have a total number of $8N$ sources. In our nonlinear problem we therefore need to satisfy $8M$ equations in $8N$ unknowns. Once the approximation Ψ_N for Ψ has been obtained accurately, equation (4.15) yields immediately the temperature solution T.

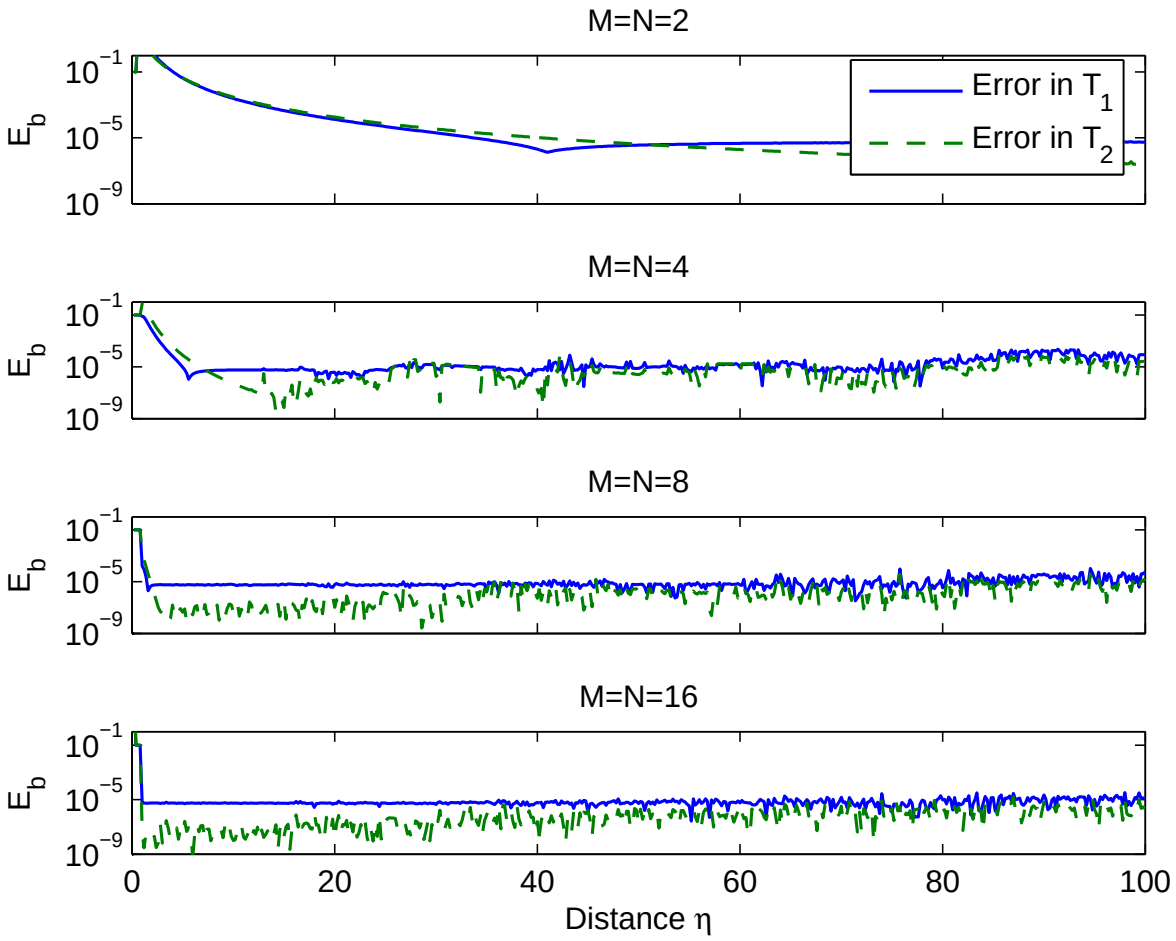

FIGURE 2. Boundary temperature error E_b versus distance η for various values of $M = N$

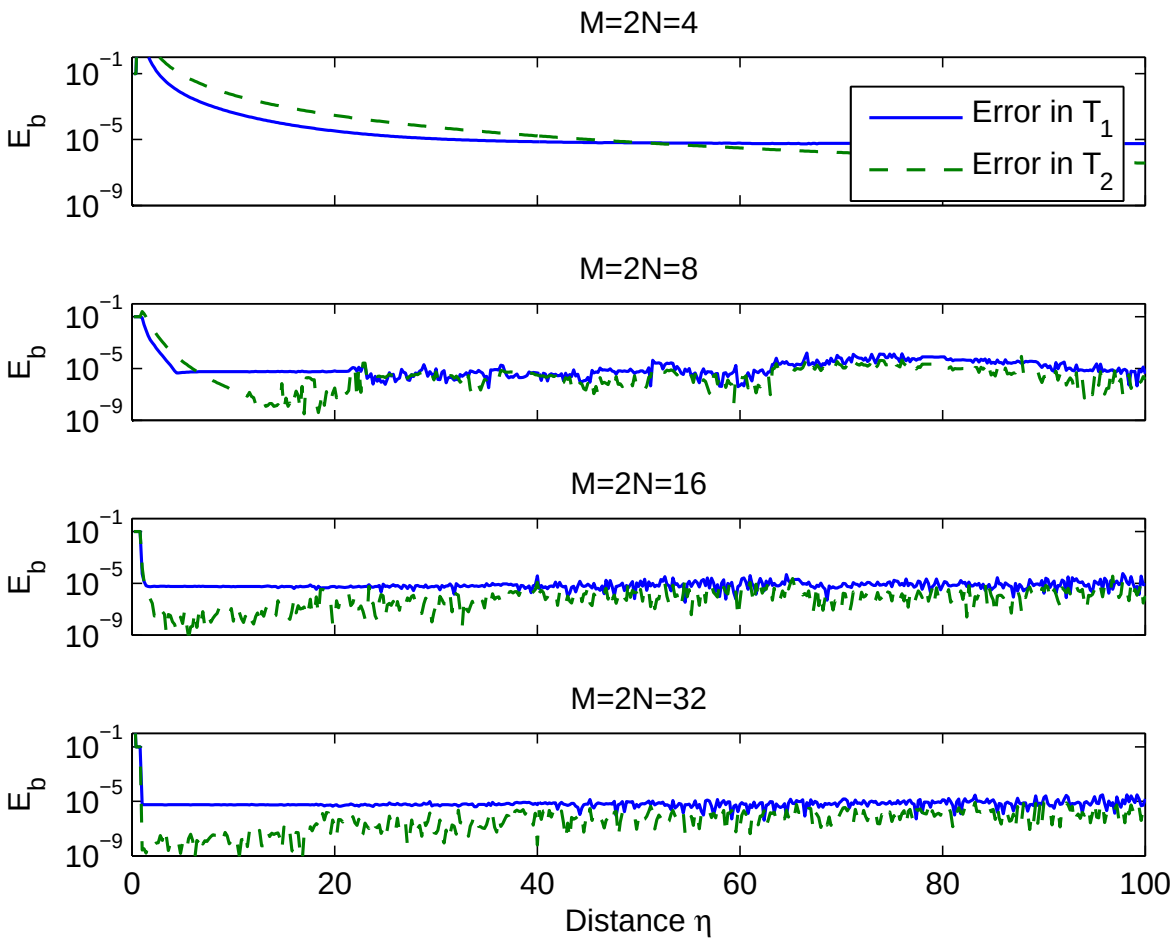

FIGURE 3. Boundary temperature error E_b versus distance η for various values of $M = 2N$

In Figure 2, we present the logarithms of the maximum errors in the boundary temperatures T_1 and T_2 versus the distance of the pseudo-boundary from the boundary for $M = N = 2, 4, 8$ and 16. These maximum errors were evaluated on 44 equally spaced points on the boundaries $\partial\Omega_1$ and $\partial\Omega_2$, respectively. Further, in Figure 3, we present the same errors for $M = 2N = 2, 4, 8$ and 16. From Figures 2 and 3 we observe that:

(i) the error E_b decreases as the distance η increases, which is consistent with the theoretical studies on the convergence of the MFS, see [24, 29];

(ii) the accuracy in predicting T_2 is better than that of T_1 possibly because the highly nonlinear radiative boundary condition is present at the upstream face AD;

(iii) the results of Figure 3 are only slightly better than those of Figure 2, implying that the increase in the ratio of boundary points to singularities has little effect on the accuracy of the method. This is consistent with the observations reported in [23].

In Figure 4, we present the numerical isotherms inside the solution domains Ω_1 and Ω_2, obtained with $M = N = 16$. These are in very good agreement with the analytical solutions (4.13). In Figure 5, we present the error profiles in T_1 and T_2 in Ω for $M = N = 2, 4, 8$ and 16. From this figure we can see the improvement in the accuracy as M (and N) increases. In Table 1, we present the approximations obtained for $a = T_1(0)$, $b = T_2(3)$, $c = T_1(1)$, $d = T_2(1)$

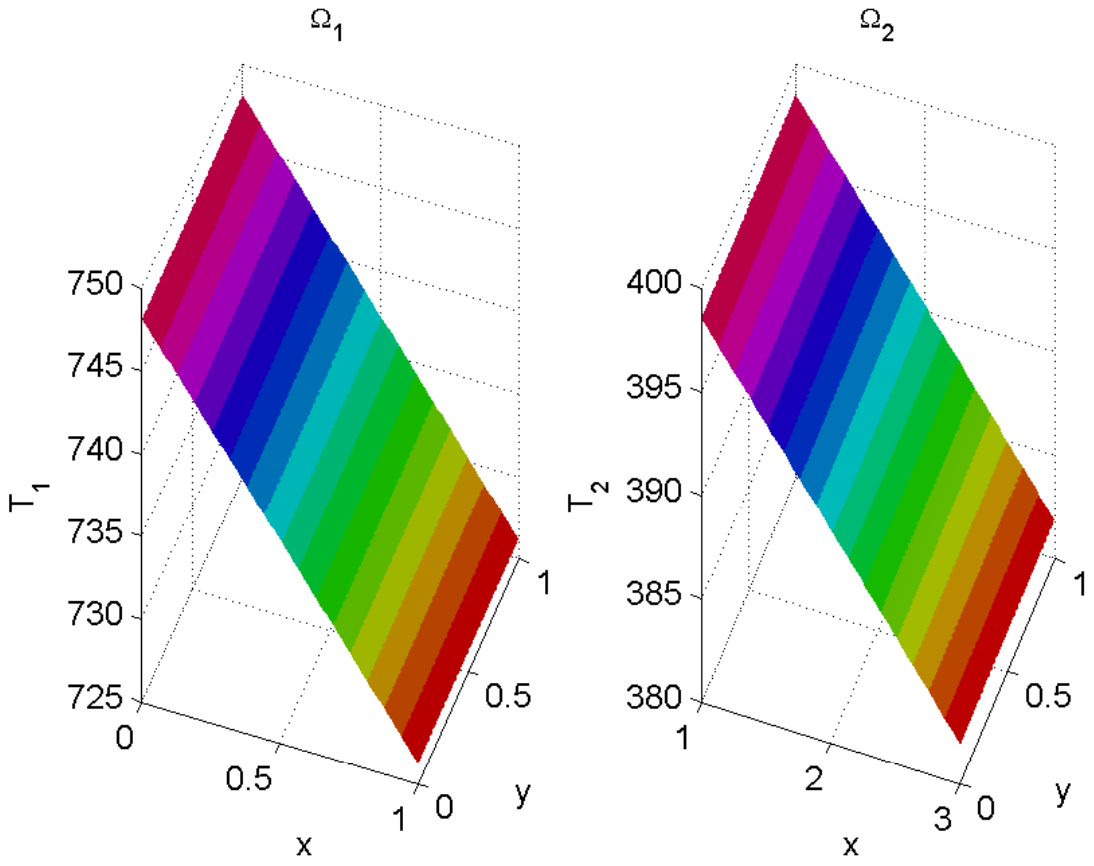

FIGURE 4. Isotherms in Ω for $M = N = 16$

$M = N$	q	a	b	c	d
2	1638.38660	748.14674	381.91861	726.21940	398.54208
4	1638.38130	748.14644	381.91916	726.21899	398.54273
8	1638.38161	748.14643	381.91908	726.21898	398.54266
16	1638.38161	748.14643	381.91908	726.21898	398.54266
Initial	1638.38161	748.14643	381.91908	726.21898	398.54266

TABLE 1. Results for constants q, a, b, c and d for various values of $M = N$

and q, for various numbers of degrees of freedom. These approximations were obtained by evaluating the MFS values at 101 equally spaced points on the corresponding vertical sides, and then taking the average. For example, in the case of a, we took

$$a = \frac{1}{101}\sum_{i=1}^{101} T_1^{MN}(0, y_i), \quad \text{where} \quad y_i = \frac{i-1}{100}, \quad i = 1, 2, \cdots 101,$$

where T_1^{MN} is the MFS approximation for T_1. Again we observe the improvement in the accuracy as the number of degrees of freedom increases.

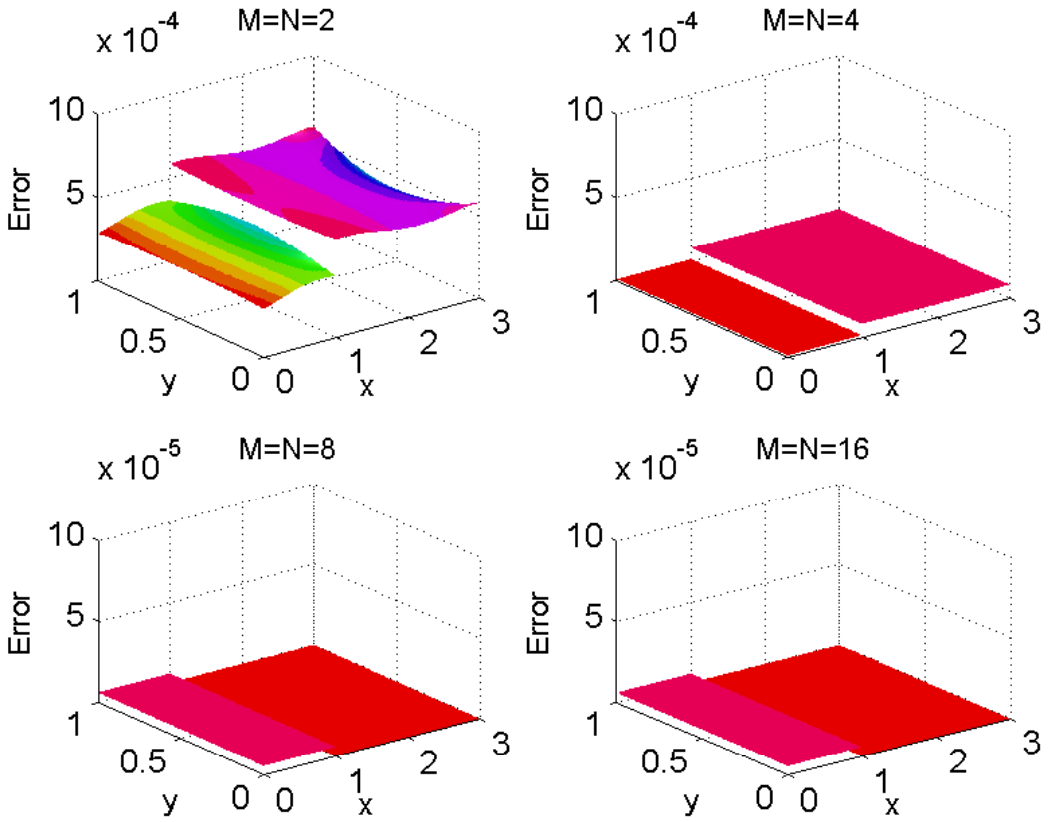

FIGURE 5. Temperature error profiles in Ω for various values of $M = N$

4.2. **Example 2.** This example is included in order to show the versatility and possible field of practical application of both the developed technique and its computer implementation. As in Example 1, the boundary conditions comprise radiation, convection, and ideal and non-ideal contact at the interface. The geometry and boundary conditions of the problem investigated in [8] using the BEM are shown in Figure 6. Unlike Example 1, the temperature field is two-dimensional and there is no analytical solution available. The composite material $\Omega = \Omega_1 \cup \Omega_2 =$ rectangle $ACFDA$ with the circular hole HG, is formed by layering the heat conductors $\Omega_1 = ABH(\text{left})GEDA$ and $\Omega_2 = BCFEG(\text{right})HB$. The thermal conductivities in each layer are linear functions of temperature given by

$$k_1(T_1) = k_{0_1}(1 + m_1(T_1)) = 70\left(1 + \frac{T_1 - 300}{1050}\right); \quad W/(mK), \tag{4.28}$$

$$k_2(T_2) = k_{0_2}(1 + m_2(T_2)) = 30\left(1 + \frac{T_2 - 300}{525}\right); \; W/(mK). \tag{4.29}$$

The sides ABC, DEF and the circular cavity HG are insulated. The front face AD exchanges heat by convection with the heat transfer coefficient $h = 30W/(m^2K)$ and $T_f = 350K$. On the back face, the radiation condition with $\epsilon = 0.4$ and $T_s = 1000K$ is prescribed. The interface GE is at ideal contact, whilst on the interface HB imperfect thermal contact with $R = 0.1m^2K/W$ is assumed.

The mathematical problem described above and depicted in Figure 6 can be written as

$$\nabla \cdot \left(70\left(1 + \frac{T_1 - 300}{1050}\right)\nabla T_1\right) = 0, \quad \text{in } \Omega_1 = ABH(\text{left})GEDA, \tag{4.30}$$

$$\nabla \cdot \left(30\left(1+\frac{T_2-300}{525}\right)\nabla T_2\right)=0, \quad \text{in } \Omega_2 = BCFEG(\text{right})HB, \tag{4.31}$$

$$\frac{\partial T_1}{\partial y}(x,0)=\frac{\partial T_1}{\partial y}(x,2)=0, \quad x\in(0,1) \quad (\text{on } AB\cup DE), \tag{4.32}$$

$$\frac{\partial T_2}{\partial y}(x,0)=\frac{\partial T_2}{\partial y}(x,2)=0, \quad x\in(1,3) \quad (\text{on } BC\cup EF), \tag{4.33}$$

$$70\left(1+\frac{T_1(0,y)-300}{1050}\right)\frac{\partial T_1}{\partial x}(0,y)=30(T_1(0,y)-350), \quad y\in(0,2) \quad (\text{on } AD), \tag{4.34}$$

$$-30\left(1+\frac{T_2(3,y)-300}{525}\right)\frac{\partial T_2}{\partial x}(3,y)=2.268204\times 10^{-8}(T_2^4(3,y)-10^{12}),\ y\in(0,2) \quad (\text{on } CF), \tag{4.35}$$

$$T_1(1,y)=T_2(1,y)-7\left(1+\frac{T_1(1,y)-300}{1050}\right)\frac{\partial T_1}{\partial x}(1,y), \quad y\in(1.5,2) \quad (\text{on } HB), \tag{4.36}$$

$$T_1(1,y)=T_2(1,y), \quad y\in(0,0.5) \quad (\text{on } GE), \tag{4.37}$$

$$70\left(1+\frac{T_1(1,y)-300}{1050}\right)\frac{\partial T_1}{\partial x}(1,y)=30\left(1+\frac{T_2(1,y)-300}{525}\right)\frac{\partial T_2}{\partial x}(1,y),\ y\in(0,0.5)\cup(1.5,2)\ (\text{on } HB\cup GE), \tag{4.38}$$

$$(x-1)\frac{\partial T_1}{\partial x}+(y-1)\frac{\partial T_1}{\partial y}=0, \quad \text{on } HG(\text{left}), \tag{4.39}$$

$$(x-1)\frac{\partial T_2}{\partial x}+(y-1)\frac{\partial T_2}{\partial y}=0, \quad \text{on } HG(\text{right}). \tag{4.40}$$

In (4.39) and (4.40)

$$HG(\text{left})=\{(x,y)|(x-1)^2+(y-1)^2=1/4,\ 0.5\le x\le 1\}, \tag{4.41}$$

$$HG(\text{right})=\{(x,y)|(x-1)^2+(y-1)^2=1/4,\ 1< x\le 1.5\}, \tag{4.42}$$

Employing transformation (2.9) yields

$$\Psi_1=\psi_1(T_1)=\frac{150\,T_1+0.1\,T_1^2}{210}, \quad \Psi_2=\psi_2(T_2)=\frac{45\,T_2+0.1\,T_2^2}{105}, \tag{4.43}$$

while the inverses of (4.43) are given by

$$T_1=\frac{\sqrt{5625+21\,\Psi_1}-75}{0.1}, \quad T_2=\frac{\sqrt{2025+42\,\Psi_2}-45}{0.2}. \tag{4.44}$$

In the Kirchhoff transform space, problem (4.30)-(4.40) becomes

$$\nabla^2\Psi_1=0, \quad \text{in } \Omega_1 = ABH(\text{left})GEDA, \tag{4.45}$$

$$\nabla^2\Psi_2=0, \quad \text{in } \Omega_2 = BCFEG(\text{right})HB, \tag{4.46}$$

$$\frac{\partial \Psi_1}{\partial y}(x,0)=\frac{\partial \Psi_1}{\partial y}(x,2)=0, \quad x\in(0,1) \quad (\text{on } AB\cup DE), \tag{4.47}$$

$$\frac{\partial \Psi_2}{\partial y}(x,0)=\frac{\partial \Psi_2}{\partial y}(x,2)=0, \quad x\in(1,3) \quad (\text{on } BC\cup EF), \tag{4.48}$$

$$7\,\frac{\partial \Psi_1}{\partial x}(0,y)=30\,(\sqrt{5625+21\,\Psi_1(0,y)}-110), \quad y\in(0,2) \quad (\text{on } AD), \tag{4.49}$$

$$-\frac{\partial \Psi_2}{\partial x}(3,y)=0.756068\times 10^{-5}\left[\left(\frac{\sqrt{2025+42\,\Psi_2(3,y)}-45}{2}\right)^4-10^8\right], y\in(0,2) \quad (\text{on } CF), \tag{4.50}$$

$$\frac{\sqrt{5625+21\,\Psi_1(1,y)}-75}{0.1}=\frac{\sqrt{2025+42\,\Psi_2(1,y)}-45}{0.2}-7\,\frac{\partial \Psi_1}{\partial x}(1,y), y\in(1.5,2) \quad (\text{on } HB), \tag{4.51}$$

$$\frac{\sqrt{5625+21\,\Psi_1(1,y)}-75}{0.1}=\frac{\sqrt{2025+42\,\Psi_2(1,y)}-45}{0.2}, \quad y\in(0,0.5) \quad (\text{on } GE), \tag{4.52}$$

$$7\,\frac{\partial \Psi_1}{\partial x}(1,y)=3\,\frac{\partial \Psi_2}{\partial x}(1,y), y\in(0,0.5)\cup(1.5,2) \quad (\text{on } HB\cup GE), \tag{4.53}$$

$$(x-1)\,\frac{\partial \Psi_1}{\partial x}+(y-1)\,\frac{\partial \Psi_1}{\partial y}=0, \quad \text{on } HG(\text{left}), \tag{4.54}$$

$$(x-1)\,\frac{\partial \Psi_2}{\partial x}+(y-1)\,\frac{\partial \Psi_2}{\partial y}=0, \quad \text{on } HG(\text{right}). \tag{4.55}$$

In the MFS discretization of problem (4.45)-(4.55), we take M collocation points on each of the segments AD, DE, AB and GH(left) of $\partial\Omega_1$, M collocation points on each of the segments EF, FC, CB and GH(right) of $\partial\Omega_2$, and $M/2$ collocation points on each of the segments EG and HB of the interface Γ_{12}. The total number of equations to be satisfied is therefore $10M$. Thus the nonlinear least-squares functional (3.3) is given by

$$\begin{aligned}
S(\boldsymbol{c}^1,\boldsymbol{c}^2) = &\sum_{i=1}^{2}\left\{\sum_{j=1}^{2M}\left[\frac{\partial \Psi^i_{\mathcal{N}}}{\partial y}(\boldsymbol{c}^i,\boldsymbol{\xi}^i;\boldsymbol{x}^i_j)\right]^2\right\}+\sum_{j=2M+1}^{3M}\left[7\frac{\partial \Psi^1_{\mathcal{N}}}{\partial x}(\boldsymbol{c}^1,\boldsymbol{\xi}^1;\boldsymbol{x}^1_j)-30(\sqrt{5625+21\Psi^1_{\mathcal{N}}(\boldsymbol{c}^1,\boldsymbol{\xi}^1;\boldsymbol{x}^1_j)}-110)\right]^2\\
&+\sum_{j=2M+1}^{3M}\left\{\frac{\partial \Psi^2_{\mathcal{N}}}{\partial x}(\boldsymbol{c}^2,\boldsymbol{\xi}^2;\boldsymbol{x}^2_j)+0.756068\times 10^{-5}\left[\left(\frac{\sqrt{2025+42\Psi^2_{\mathcal{N}}(\boldsymbol{c}^2,\boldsymbol{\xi}^2;\boldsymbol{x}^2_j)}-45}{2}\right)^4-10^8\right]\right\}^2\\
&+\sum_{i=1}^{2}\left\{\sum_{j=3M+1}^{4M}\left[(x^i_j-1)\frac{\partial \Psi^i_{\mathcal{N}}}{\partial x}(\boldsymbol{c}^i,\boldsymbol{\xi}^i;\boldsymbol{x}^i_j)+(y^i_j-1)\frac{\partial \Psi^i_{\mathcal{N}}}{\partial y}(\boldsymbol{c}^i,\boldsymbol{\xi}^i;\boldsymbol{x}^i_j)\right]^2\right\}\\
&+\sum_{j=1}^{M}\left[7\frac{\partial \Psi^1_{\mathcal{N}}}{\partial x}(\boldsymbol{c}^1,\boldsymbol{\xi}^1;\boldsymbol{x}_j)-3\frac{\partial \Psi^2_{\mathcal{N}}}{\partial x}(\boldsymbol{c}^2,\boldsymbol{\xi}^2;\boldsymbol{x}_j)\right]^2\\
&+\sum_{j=1}^{M/2}\left[\frac{\sqrt{5625+21\Psi^1_{\mathcal{N}}(\boldsymbol{c}^1,\boldsymbol{\xi}^1;\boldsymbol{x}_j)}-75}{0.1}-\frac{\sqrt{2025+42\Psi^2_{\mathcal{N}}(\boldsymbol{c}^2,\boldsymbol{\xi}^2;\boldsymbol{x}_j)}-45}{0.2}\right]^2\\
&+\sum_{j=M/2+1}^{M}\left[\frac{\sqrt{5625+21\Psi^1_{\mathcal{N}}(\boldsymbol{c}^1,\boldsymbol{\xi}^1;\boldsymbol{x}_j)}-75}{0.1}-\frac{\sqrt{2025+42\Psi^2_{\mathcal{N}}(\boldsymbol{c}^2,\boldsymbol{\xi}^2;\boldsymbol{x}_j)}-45}{0.2}+7\frac{\partial \Psi^1_{\mathcal{N}}}{\partial x}(\boldsymbol{c}^1,\boldsymbol{\xi}^1;\boldsymbol{x}_j)\right]^2,
\end{aligned} \tag{4.56}$$

where the boundary collocation points are given by

$$\boldsymbol{x}^1_j=\left(\frac{j}{M+1},0\right), \quad \boldsymbol{x}^1_{M+j}=\left(\frac{j}{M+1},2\right), \quad \boldsymbol{x}^1_{2M+j}=\left(0,\frac{2(j-1)}{M-1}\right), \tag{4.57}$$

$$\boldsymbol{x}^1_{3M+j}=\left(1+\frac{1}{2}\cos\left(\frac{\pi}{2}+\frac{\pi j}{M+1}\right),1+\frac{1}{2}\sin\left(\frac{\pi}{2}+\frac{\pi j}{M+1}\right)\right), \tag{4.58}$$

$$\boldsymbol{x}^2_j=\left(1+\frac{2j}{M+1},0\right), \quad \boldsymbol{x}^2_{M+j}=\left(1+\frac{2j}{M+1},2\right), \quad \boldsymbol{x}^2_{2M+j}=\left(3,\frac{2(j-1)}{M-1}\right), \tag{4.59}$$

$$\boldsymbol{x}^2_{3M+j}=\left(1+\frac{1}{2}\cos\left(-\frac{\pi}{2}+\frac{\pi j}{M+1}\right),1+\frac{1}{2}\sin\left(-\frac{\pi}{2}+\frac{\pi j}{M+1}\right)\right), \qquad j=\overline{1,M}, \tag{4.60}$$

and

$$\boldsymbol{x}_j=\left(1,\frac{j-1}{M-2}\right), \quad \boldsymbol{x}_{M/2+j}=\left(1,1.5+\frac{j-1}{M-2}\right), \quad j=\overline{1,M/2}. \tag{4.61}$$

The presence of an insulated circular cavity prevents the temperature from being one-dimensional. Once the approximation Ψ_N for Ψ is calculated, the temperature solution is readily obtained from equation (4.44). As in the case of Example 1, the source points are located on pseudo-boundaries $\partial\Omega_1'$ and $\partial\Omega_2'$ which enclose and are similar to the domains Ω_1 and Ω_2, respectively, at a distance $\eta>0$ from them. On each pseudo-boundary the sources are distributed in a similar way to the distribution of the boundary points. More specifically, we take N source points on each of the segments of $\partial\Omega_1'$ which correspond to AD, DE, AB and GH(left), and $N/2$ source points on each of the segments that correspond to EG and HB. On $\partial\Omega_2'$, we take N source points on each of the segments which

correspond to EF, FC, CB and GH(right) and $N/2$ source points on each of the segments that correspond to EG and HB. Thus the total number of sources is $2\mathcal{N} = 10N$. A typical distribution of boundary points and sources, for each subdomain is depicted in Figure 7.

In Figure 8, we present the logarithms of the maximum relative errors in the satisfaction of the boundary conditions for $M = N = 4, 8, 12, 16$ and 24. These maximum errors were evaluated on 96 equally spaced points on the boundaries of each subregion. From this figure we observe that as $M = N$ increases the maximum error decreases. The two- and three-dimensional isotherms obtained with $M = N = 24$ are presented in Figures 9 and 10, respectively. These are in very good agreement with the corresponding results of [7] obtained using the BEM. As expected, there is a jump in the temperature field along imperfectly contact interface HB, whereas at the remaining portion of the ideal contact interface EG the temperature field is smooth.

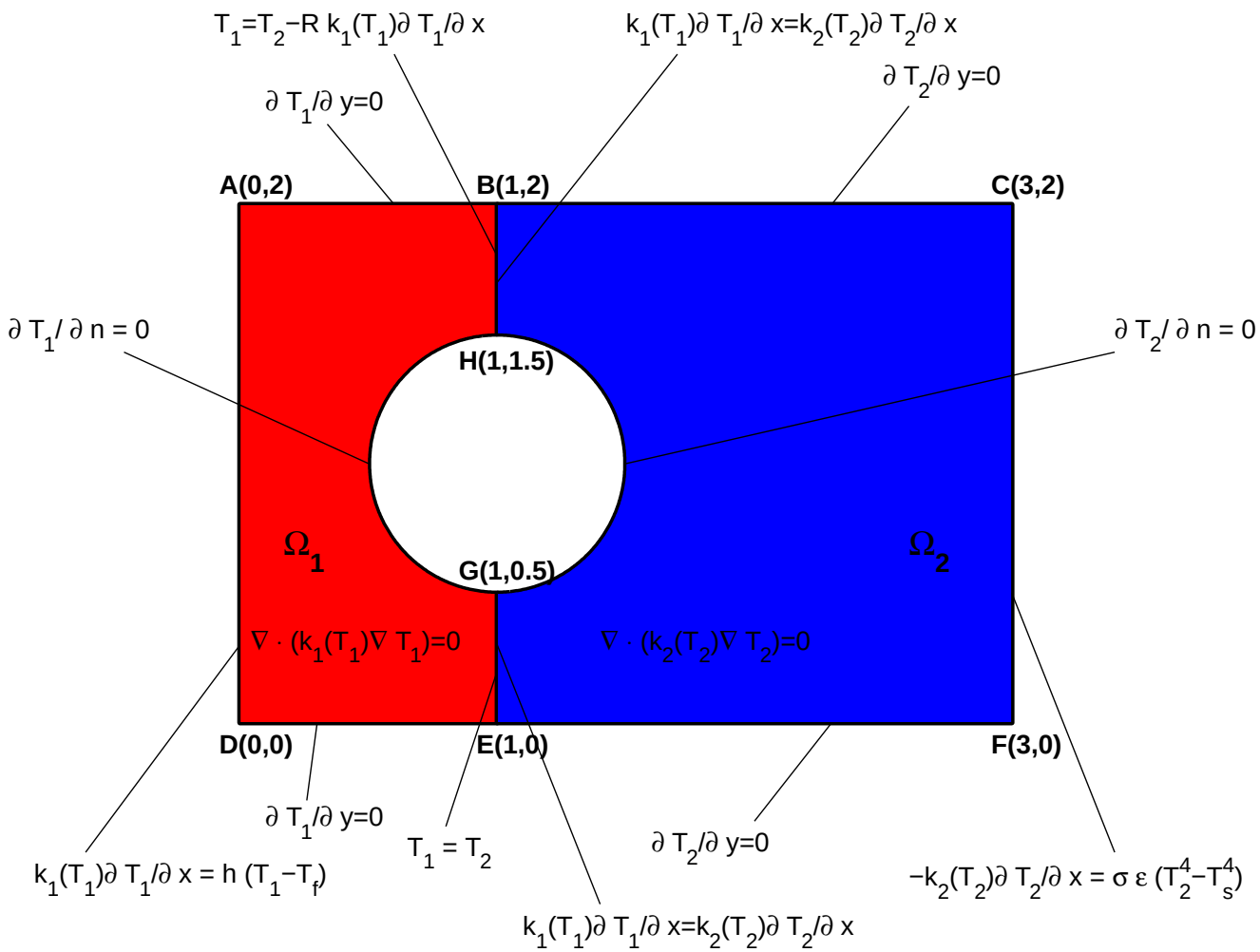

FIGURE 6. Geometry and boundary conditions for Example 2

4.3. **Example 3.** The two examples considered so far have been two-dimensional and the materials possessed thermal conductivities which varied linearly with the temperature. In this example we consider a case when the thermal conductivity of one of the two layers varies nonlinearly with the temperature. More precisely, let

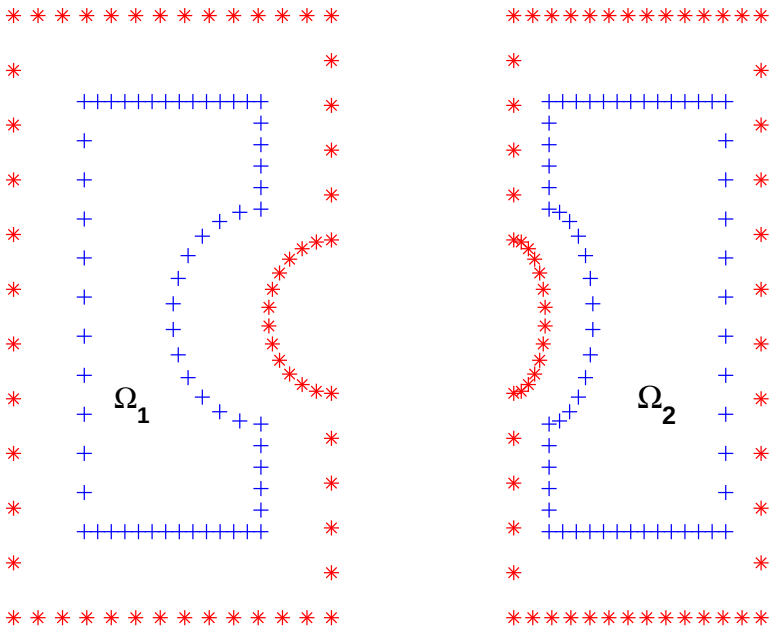

FIGURE 7. Typical distribution of boundary points (+) and sources (∗) in Example 2

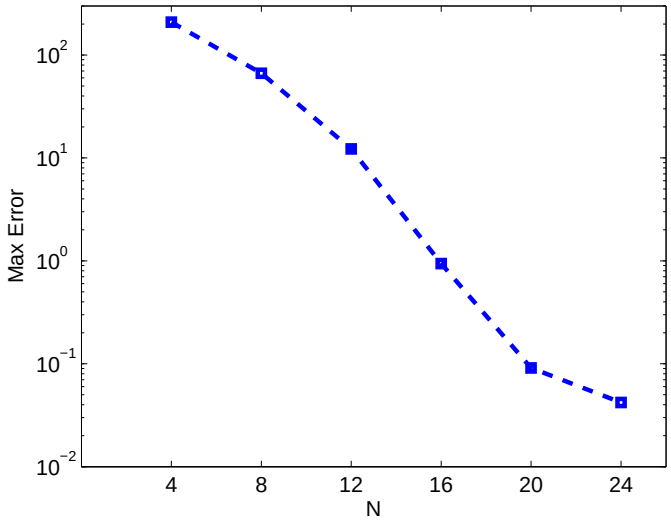

FIGURE 8. Convergence of maximum error in the satisfaction of boundary conditions for Example 2

$\Omega_1 = (0,1) \times (0,1)$, $\Omega_2 = (0,1) \times (-1,0)$ and take $k_1(T_1) = 1 + e^{T_1}$, $k_2(T_2) = 2$.

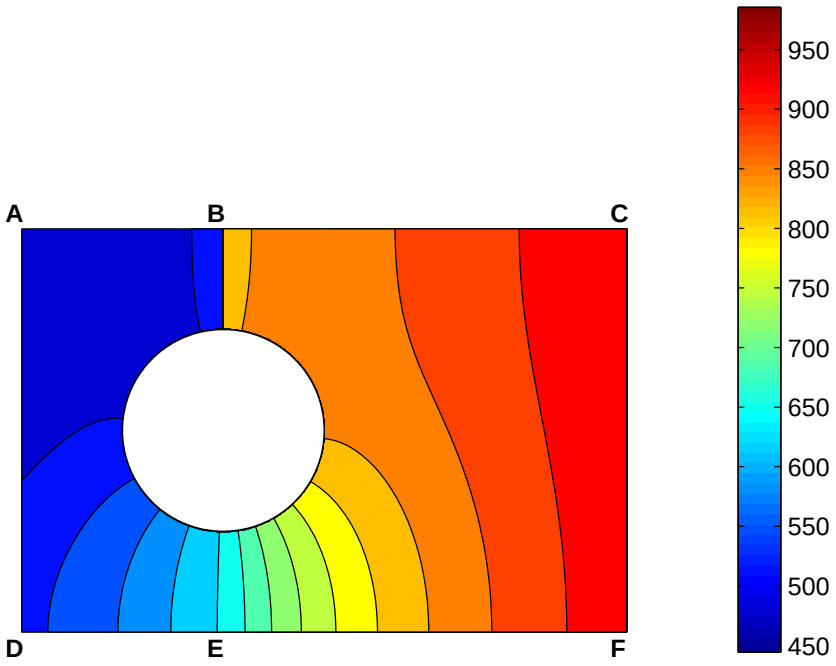

FIGURE 9. Two-dimensional isotherm map for Example 2

We consider the problem (Figure 11)

$$\nabla \cdot \left((1+e^{T_1})\nabla T_1\right) = 0, \quad \text{in} \quad \Omega_1, \tag{4.62}$$

$$\nabla^2 T_2 = 0, \quad \text{in} \quad \Omega_2, \tag{4.63}$$

$$-\left(1+e^{T_1(0,y)}\right)\frac{\partial T_1}{\partial x}(0,y) = -y, \quad y \in (0,1], \tag{4.64}$$

$$\left(1+e^{T_1(x,1)}\right)\frac{\partial T_1}{\partial y}(x,1) = x, \quad x \in (0,1], \tag{4.65}$$

$$\left(1+e^{T_1(1,y)}\right)\frac{\partial T_1}{\partial x}(1,y) = y, \quad y \in (0,1), \tag{4.66}$$

$$T_2(0,y) = 0, \quad y \in [-1,0), \tag{4.67}$$

$$T_2(x,-1) = -x/2, \quad x \in [0,1), \tag{4.68}$$

$$T_2(1,y) = y/2, \quad y \in [-1,0), \tag{4.69}$$

$$T_1(x,0) = T_2(x,0), \quad x \in [0,1], \tag{4.70}$$

$$(1+e^{T_1(x,0)})\frac{\partial T_1}{\partial y}(x,0) = 2\frac{\partial T_2}{\partial y}(x,0), \quad x \in (0,1). \tag{4.71}$$

Then upon the Kirchhoff transformations (2.9)

$$\Psi_1 = \psi_1(T_1) = T_1 + e^{T_1} - 1, \tag{4.72}$$

$$\Psi_2 = \psi_2(T_2) = T_2, \tag{4.73}$$

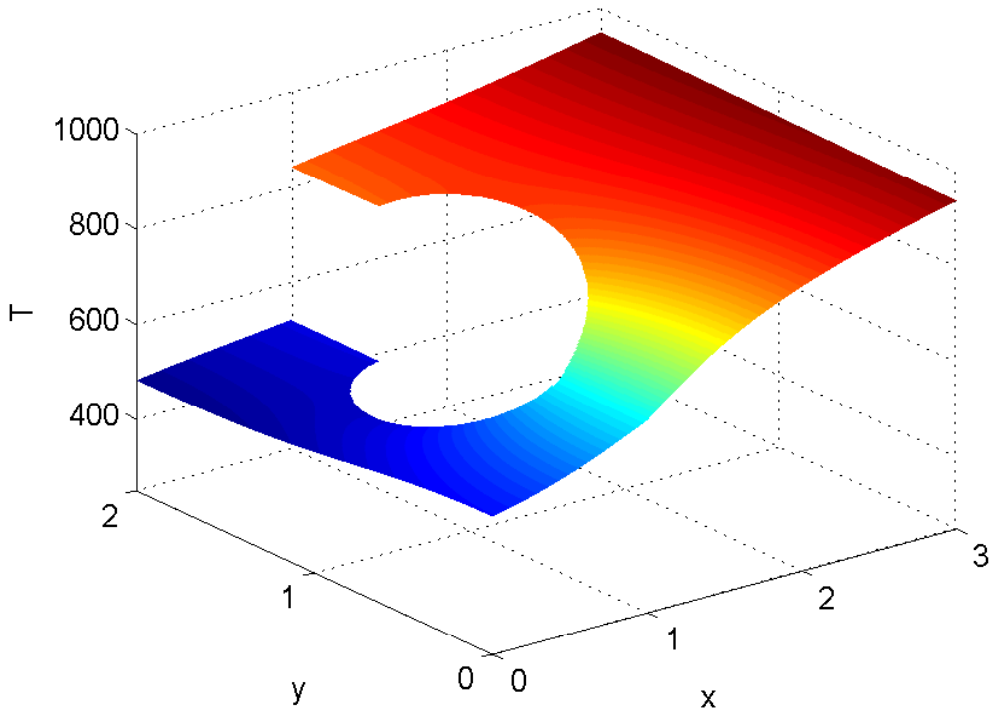

FIGURE 10. Three-dimensional isotherm map for Example 2

the problem (4.62)-(4.71) transforms into

$$\nabla^2 \Psi_1 = 0, \quad \text{in} \quad \Omega_1, \tag{4.74}$$

$$\nabla^2 \Psi_2 = 0, \quad \text{in} \quad \Omega_2, \tag{4.75}$$

$$-\frac{\partial \Psi_1}{\partial x}(0,y) = -y, \quad y \in (0,1], \tag{4.76}$$

$$\frac{\partial \Psi_1}{\partial y}(x,1) = x, \quad x \in (0,1], \tag{4.77}$$

$$\frac{\partial \Psi_1}{\partial x}(1,y) = y, \quad y \in (0,1), \tag{4.78}$$

$$\Psi_2(0,y) = 0, \quad y \in [-1,0), \tag{4.79}$$

$$\Psi_2(x,-1) = -x, \quad x \in [0,1), \tag{4.80}$$

$$\Psi_2(1,y) = y, \quad y \in [-1,0), \tag{4.81}$$

$$\psi_1^{-1}(\Psi_1(x,0)) = \Psi_2(x,0), \quad x \in [0,1], \tag{4.82}$$

$$\frac{\partial \Psi_1}{\partial y}(x,0) = 2\,\frac{\partial \Psi_2}{\partial y}(x,0), \quad x \in (0,1). \tag{4.83}$$

We solve problem (4.74)-(4.83) using the MFS with condition (4.82) replaced by

$$\Psi_1(x,0) = \Psi_2(x,0) + e^{\Psi_2(x,0)} - 1, \quad x \in [0,1] \tag{4.84}$$

and compare the numerical results with the analytical solution

$$\Psi_1(x,y) = xy, \quad (x,y) \in \Omega_1, \tag{4.85}$$

$$\Psi_2(x,y) = \frac{xy}{2}, \quad (x,y) \in \Omega_2. \tag{4.86}$$

$$\tag{4.87}$$

We placed M collocation points on each side of the squares Ω_1 and Ω_2 yielding a total of $8M$ collocations points. Similarly, we placed N sources on each side of each of the pseudoboundaries $\partial\Omega_1'$ and $\partial\Omega_2'$. In particular, we took

$$\boldsymbol{x}_j^1 = \left(0, \frac{j-1}{M-1}\right), \quad \boldsymbol{x}_j^2 = \left(0, -\frac{j-1}{M-1}\right), \tag{4.88}$$

$$\boldsymbol{x}_{M+j}^1 = \left(\frac{j}{M+1}, 1\right), \quad \boldsymbol{x}_{M+j}^2 = \left(\frac{j}{M+1}, -1\right), \tag{4.89}$$

$$\boldsymbol{x}_{2M+j}^1 = \left(1, 1-\frac{j-1}{M-1}\right), \quad \boldsymbol{x}_{2M+j}^2 = \left(1, -1+\frac{j-1}{M-1}\right), \tag{4.90}$$

and

$$\boldsymbol{x}_j = \left(\frac{j}{M+1}, 0\right), \qquad j = \overline{1, M}. \tag{4.91}$$

The nonlinear least-squares objective function (3.3) takes the form

$$\begin{aligned} S(\boldsymbol{c}^1, \boldsymbol{c}^2) = \sum_{j=1}^{3M} \left[\Psi_{\mathcal{N}}^2(\boldsymbol{c}^2, \boldsymbol{\xi}^2; \boldsymbol{x}_j^2) - \Psi_2(\boldsymbol{x}_j^2)\right]^2 + \sum_{j=1}^{3M} \left[\frac{\partial \Psi_{\mathcal{N}}^1}{\partial n}(\boldsymbol{c}^1, \boldsymbol{\xi}^1; \boldsymbol{x}_j^1) - \frac{\partial \Psi_1(\boldsymbol{x}_j^1)}{\partial n}\right]^2 \\ + \sum_{j=1}^{M} \left[\Psi_{\mathcal{N}}^1(\boldsymbol{c}^1, \boldsymbol{\xi}^1; \boldsymbol{x}_j) - \Psi_{\mathcal{N}}^2(\boldsymbol{c}^2, \boldsymbol{\xi}^2; \boldsymbol{x}_j) - e^{\Psi_{\mathcal{N}}^2(\boldsymbol{c}^2, \boldsymbol{\xi}^2; \boldsymbol{x}_j)} + 1,\right]^2 \\ + \sum_{j=1}^{M} \left[\frac{\partial \Psi_{\mathcal{N}}^1}{\partial y}(\boldsymbol{c}^1, \boldsymbol{\xi}^1; \boldsymbol{x}_j) - 2\,\frac{\partial \Psi_{\mathcal{N}}^2}{\partial y}(\boldsymbol{c}^2, \boldsymbol{\xi}^2; \boldsymbol{x}_j)\right]^2. \end{aligned} \tag{4.92}$$

After solving boundary value problem (4.74)-(4.83) for $\Psi_{\mathcal{N}}^1$ and $\Psi_{\mathcal{N}}^2$, to recover $T_1(\boldsymbol{x})$ for each $\boldsymbol{x} \in \Omega_1$ we need to solve numerically the nonlinear equation

$$T_1(\boldsymbol{x}) + e^{T_1(\boldsymbol{x})} - 1 = \Psi_{\mathcal{N}}^1(\boldsymbol{c}^1, \boldsymbol{\xi}^1; \boldsymbol{x}) \tag{4.93}$$

which always has a unique solution since the function $F : \mathbb{R} \to \mathbb{R}$, $f(a) = a + e^a - 1$ is bijective and strictly increasing. This can be done using the `matlab` function `fzero` which finds a zero of a function of one variable.

The absolute error in T_2 was calculated on a uniform 20×20 grid in Ω_2 and in Figure 12 we present the absolute error profiles for $M = N = 2, 4$ and 8. As the number of degrees of freedom increases, the error decreases.

Further, in Figure 13 we present a plot of the isotherms throughout the whole of the composite solution domain $\Omega_1 \cup \Omega_2$. Note that there is no closed form analytical solution for $T_1(x, y)$ available to compare with.

In cases of thermal conductivities whose primitive (indefinite integral) cannot be calculated explicitly, such as $k(T) = e^{T^2}$, the integral in the Kirchhoff transformation has to be calculated numerically. However, such conductivity variations are seldom encountered in the engineering practice. It is more likely, that in such cases one first approximates $k(T)$ by a piecewise linear function and then applies the Kirchhoff transformation over each linear portion [2], as described globally for Examples 1 and 2. The same piecewise linear approximation can be adopted if the thermal conductivity is given at a set of discrete nodes rather than as an explicit function.

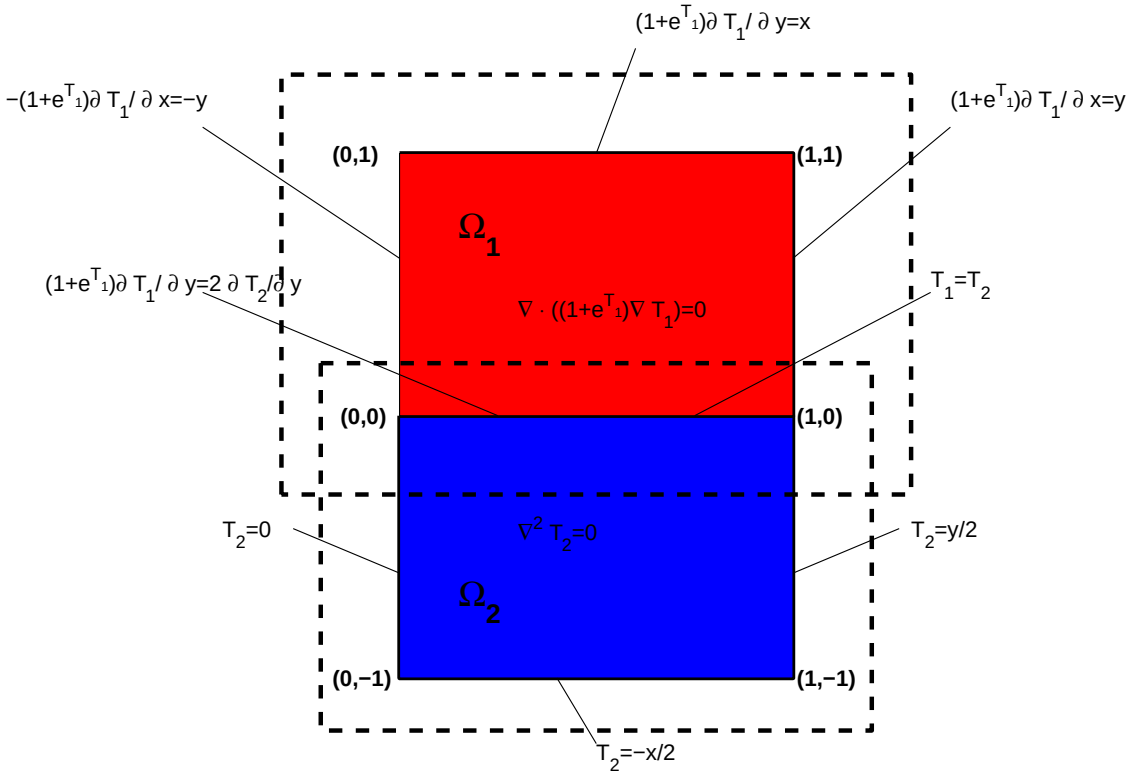

FIGURE 11. Geometry and boundary conditions for Example 3

4.4. **Example 4.** The examples considered so far have been two-dimensional. In this example, we consider a three-dimensional composite heat conductor formed with two layers of material $\Omega_1 = (0,1)\times(0,1)\times(0,1)$ and $\Omega_2 = (0,1)\times(0,1)\times(-1,0)$ as shown in Figure 14. Further, we consider that the layer Ω_1 has a thermal conductivity which varies exponentially with the temperature, namely, see e.g. [31],

$$k_1(T_1) = \mathrm{e}^{T_1}, \tag{4.94}$$

whilst the other layer Ω_2 is homogeneous with uniform thermal conductivity

$$k_2(T_2) = 1. \tag{4.95}$$

We consider the problem

$$\nabla\cdot\left(\mathrm{e}^{T_1}\,\nabla T_1\right) = 0, \qquad \text{in} \qquad \Omega_1 = (0,1)\times(0,1)\times(0,1), \tag{4.96}$$

$$\nabla^2 T_2 = 0, \qquad \text{in} \qquad \Omega_2 = (0,1)\times(0,1)\times(-1,0) \tag{4.97}$$

with interface conditions

$$T_1(x,y,0) = T_2(x,y,0), \qquad (x,y)\in[0,1]\times[0,1], \tag{4.98}$$

$$\mathrm{e}^{T_1(x,y,0)}\,\frac{\partial T_1}{\partial z}(x,y,0) = \frac{\partial T_2}{\partial z}(x,y,0), \qquad (x,y)\in[0,1]\times[0,1], \tag{4.99}$$

and subject to Dirichlet boundary conditions (2.2) given by

$$T_1(x,0,z) = \ln(2+x+z), \qquad T_1(0,y,z) = \ln(2+y+z),$$

$$T_1(x,1,z) = \ln(3+x+z), \qquad T_1(1,y,z) = \ln(3+y+z),$$

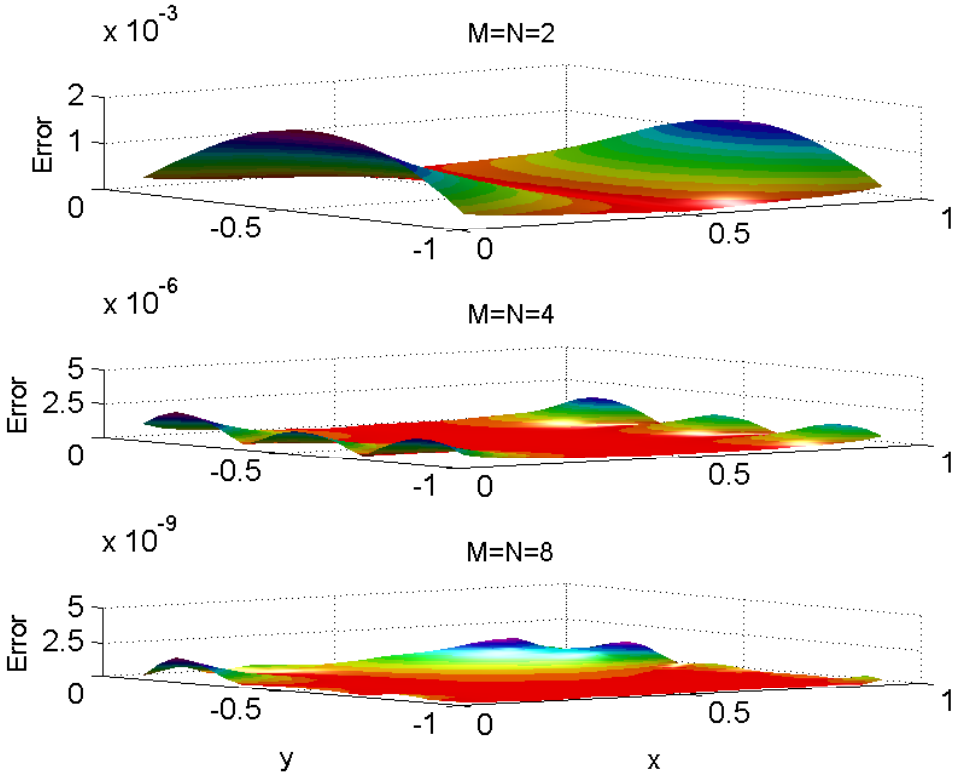

FIGURE 12. Absolute error profiles for T_2 in for Example 3

$$T_1(x,y,1) = \ln(3+x+y), \qquad (x,y,z) \in [0,1]\times[0,1]\times[0,1], \tag{4.100}$$

and

$$T_2(x,0,z) = z + \ln(2+x) + \frac{1}{2}\ln\left(1+\frac{2z^2}{(2+x)^2}\right), \qquad T_2(0,y,z) = z + \ln(2+y) + \frac{1}{2}\ln\left(1+\frac{2z^2}{(2+y)^2}\right),$$

$$T_2(x,1,z) = z + \ln(3+x) + \frac{1}{2}\ln\left(1+\frac{2z^2}{(3+x)^2}\right), \qquad T_2(1,y,z) = z + \ln(3+y) + \frac{1}{2}\ln\left(1+\frac{2z^2}{(3+y)^2}\right),$$

$$T_2(x,y,-1) = -1 + \ln(2+x+y) + \frac{1}{2}\ln\left(1+\frac{2}{(2+x+y)^2}\right), \qquad (x,y,z) \in [0,1]\times[-1,0]. \tag{4.101}$$

The boundary value problem (4.96)-(4.101) has the analytical solution

$$T_1(x,y,z) = \ln(2+x+y+z), \quad (x,y,z) \quad \text{in} \quad \Omega_1, \tag{4.102}$$

$$T_2(x,y,z) = z + \ln(2+x+y) + \frac{1}{2}\left(1+\frac{2z^2}{(2+x+y)^2}\right), \quad (x,y,z) \quad \text{in} \quad \Omega_2. \tag{4.103}$$

Employing the Kirchhoff transformation (2.9) we obtain

$$\Psi_1 = \psi_1(T_1) = \mathrm{e}^{T_1} - 1, \qquad \Psi_2 = \psi_2(T_2) = T_2\,, \tag{4.104}$$

with the inverses of (4.104) given by

$$T_1 = \ln(\Psi_1 + 1), \qquad T_2 = \Psi_2\,. \tag{4.105}$$

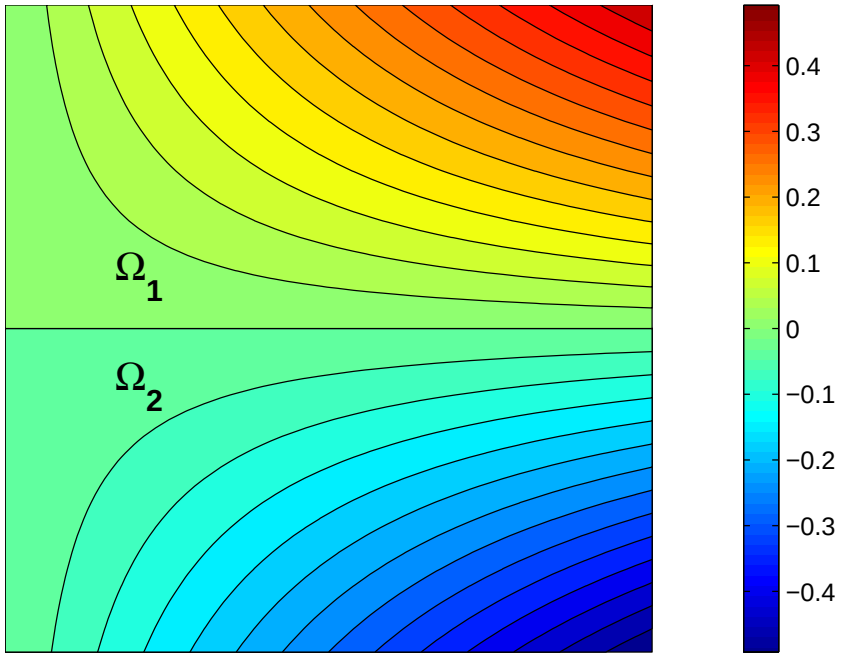

FIGURE 13. Two-dimensional isotherm map for Example 3

In the Kirchhoff transform space, problem (4.96)-(4.101) becomes

$$\nabla^2\Psi_1 = 0, \qquad \text{in} \quad \Omega_1, \tag{4.106}$$

$$\nabla^2\Psi_2 = 0, \qquad \text{in} \quad \Omega_2, \tag{4.107}$$

$$\ln\left(\Psi_1(x,y,0)+1\right) = \Psi_2(x,y,0), \qquad (x,y)\in[0,1]\times[0,1], \tag{4.108}$$

$$\frac{\partial\Psi_1}{\partial z}(x,y,0) = \frac{\partial\Psi_2}{\partial z}(x,y,0), \qquad (x,y)\in[0,1]\times[0,1], \tag{4.109}$$

with

$$\begin{aligned} &\Psi_1(x,0,z) = 1+x+z, \qquad \Psi_1(0,y,z) = 1+y+z,\\ &\Psi_1(x,1,z) = 2+x+z, \qquad \Psi_1(1,y,z) = 2+y+z,\\ &\Psi_1(x,y,1) = 2+x+y, \qquad (x,y,z)\in[0,1]\times[0,1]\times[0,1], \end{aligned} \tag{4.110}$$

and

$$\Psi_2(x,0,z) = z+\ln(2+x)+\frac{1}{2}\ln\left(1+\frac{2z^2}{(2+x)^2}\right), \qquad \Psi_2(0,y,z) = z+\ln(2+y)+\frac{1}{2}\ln\left(1+\frac{2z^2}{(2+y)^2}\right),$$

$$\Psi_2(x,1,z) = z+\ln(3+x)+\frac{1}{2}\ln\left(1+\frac{2z^2}{(3+x)^2}\right), \qquad \Psi_2(1,y,z) = z+\ln(3+y)+\frac{1}{2}\ln\left(1+\frac{2z^2}{(3+y)^2}\right),$$

$$\Psi_2(x,y,-1) = -1+\ln(2+x+y)+\frac{1}{2}\ln\left(1+\frac{2}{(2+x+y)^2}\right), \quad (x,y,z)\in[0,1]\times[0,1]\times[-1,0]. \tag{4.111}$$

The boundary value problem (4.106)-(4.111) has the analytical solution

$$\Psi_1(x,y,z) = 1 + x + y + z, \quad \text{in} \quad \Omega_1, \tag{4.112}$$

$$\Psi_2(x,y,z) = z + \ln(2+x+y) + \frac{1}{2}\left(1 + \frac{2z^2}{(2+x+y)^2}\right), \quad \text{in} \quad \Omega_2. \tag{4.113}$$

We chose $M \times M$ boundary collocation points on each of the faces of each cube and similarly $N \times N$ sources on the corresponding pseudoboundaries. Thus, in this case $\mathcal{M} = 6M^2$ and $\mathcal{N} = 6N^2$, yielding a total number of $2\mathcal{M} = 12M^2$ equations in $2\mathcal{N} = 12N^2$ unknowns. If the interface is denoted by Γ_{12} then the number of boundary collocation points on $\partial\Omega_i \backslash \Gamma_{12}$, $i = 1, 2$ is $\mathcal{M}_{\partial\Omega} = 5M^2$ and the number on the interface Γ_{12} of each subdomain is $\mathcal{M}_\Gamma = M^2$. Further, the boundary points on $\partial\Omega_i \backslash \Gamma_{12}$, $i = 1, 2$ are denoted by $(\boldsymbol{x}_j^i)_{j=\overline{1,\mathcal{M}_{\partial\Omega}}}$, $i = 1, 2$ while the points on the interface Γ_{12} are denoted by $(\boldsymbol{x}_j)_{j=\overline{1,\mathcal{M}_\Gamma}}$.
More precisely, we take

$$\boldsymbol{x}_\ell^1 = \left(0, \frac{i-1}{M-1}, \frac{j-1}{M-1}\right), \quad \boldsymbol{x}_\ell^2 = \left(0, \frac{i-1}{M-1}, -1 + \frac{j-1}{M-1}\right),$$

$$\boldsymbol{x}_{M^2+\ell}^1 = \left(1, \frac{i-1}{M-1}, \frac{j-1}{M-1}\right), \quad \boldsymbol{x}_{M^2+\ell}^2 = \left(1, \frac{i-1}{M-1}, -1 + \frac{j-1}{M-1}\right),$$

$$\boldsymbol{x}_{2M^2+\ell}^1 = \left(\frac{i}{M+1}, 0, \frac{j-1}{M-1}\right), \quad \boldsymbol{x}_{2M^2+\ell}^2 = \left(\frac{i}{M+1}, 0, -1 + \frac{j-1}{M-1}\right),$$

$$\boldsymbol{x}_{3M^2+\ell}^1 = \left(\frac{i}{M+1}, 1, \frac{j-1}{M-1}\right), \quad \boldsymbol{x}_{3M^2+\ell}^2 = \left(\frac{i}{M+1}, 1, -1 + \frac{j-1}{M-1}\right),$$

$$\boldsymbol{x}_{4M^2+\ell}^1 = \left(\frac{i}{M+1}, \frac{j}{M+1}, 1\right), \quad \boldsymbol{x}_{4M^2+\ell}^2 = \left(\frac{i}{M+1}, \frac{j}{M+1}, -1\right),$$

and

$$\boldsymbol{x}_\ell = \left(\frac{i}{M+1}, \frac{j}{M+1}, 0\right), \qquad i, j = \overline{1, M}, \quad \ell = (i-1)M + j\,. \tag{4.114}$$

The solutions $\Psi_i(\boldsymbol{x})$, $i = 1, 2$ are approximated by $\Psi_{\mathcal{N}}^i(\boldsymbol{c}^i, \boldsymbol{\xi}^i; \boldsymbol{x})$ defined in (3.1) with $d = 3$.

The nonlinear least-squares functional corresponding to (3.3) is given by

$$S(\boldsymbol{c}^1, \boldsymbol{c}^2) := \sum_{i=1}^{2} \left\{ \sum_{j=1}^{\mathcal{M}_{\partial\Omega}} \left[\Psi_{\mathcal{N}}^i(\boldsymbol{c}^i, \boldsymbol{\xi}^i; \boldsymbol{x}_j^i) - \Psi_i(\boldsymbol{x}_j^i)\right]^2 \right\} + \sum_{j=1}^{\mathcal{M}_\Gamma} \left[\ln\left(\Psi_{\mathcal{N}}^1(\boldsymbol{c}^1, \boldsymbol{\xi}^1; \boldsymbol{x}_j) + 1\right) - \Psi_{\mathcal{N}}^2(\boldsymbol{c}^2, \boldsymbol{\xi}^2; \boldsymbol{x}_j)\right]^2$$
$$+ \sum_{j=1}^{\mathcal{M}_\Gamma} \left[\frac{\Psi_{\mathcal{N}}^1}{\partial z}(\boldsymbol{c}^1, \boldsymbol{\xi}^1; \boldsymbol{x}_j) - \frac{\Psi_{\mathcal{N}}^2}{\partial z}(\boldsymbol{c}^2, \boldsymbol{\xi}^2; \boldsymbol{x}_j)\right]^2. \tag{4.115}$$

In Figures 15–17 we present the absolute errors in the temperature $T(x, y, z)$ on the planes $z = -0.5$, $z = 0$ and $z = 0.5$, respectively, obtained for $M = N = 4$, 6 and 8 (corresponding to $2\mathcal{M} = 192, 432$ and 768, respectively). As can be observed from each of these three figures the error diminishes as the number of degrees of freedom increases.

5. Conclusions

In this paper, the application of the MFS to steady-state nonlinear heat conduction problems in composite heat conductors has been investigated. The MFS is used in conjunction with a domain decomposition technique and the method recasts the problem as a nonlinear minimization problem. The numerical results obtained are in good agreement with the available analytical solutions showing high accuracy and stable convergence, and probably with the BEM results of [8] if these were to be corrected. Further, it is demonstrated that the current formulation of

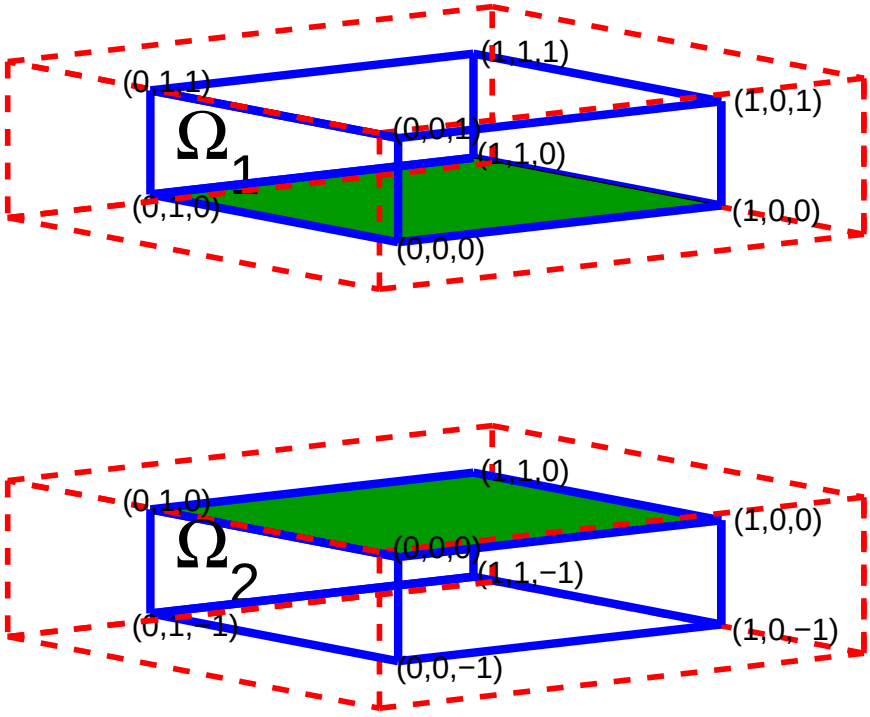

FIGURE 14. Geometry and domain decomposition for Example 4

the MFS can be easily applied to problems in irregular domains and to three-dimensional nonlinear steady-state heat conduction problems. It is also shown that the nature of the Kirchhoff transformation (and particularly its inverse) is not very restrictive and that one may easily revert to the original solution. Moreover, if a heat source is present in equation (2.1), then one can apply a modification of the MFS, as described in [18]. The proposed MFS domain decomposition technique can be implemented in a commercial code aimed at solving general convective, radiative, steady-state, nonlinear heat transfer in layered (ideal or non-ideal interface contact) heat conductors. Possible future work will concern extending the MFS analysis of [4] for linearly layered elastic materials to nonlinear elasticity.

ACKNOWLEDGEMENTS

The authors would like to thank the UK Royal Society for supporting this research.

REFERENCES

[1] C. J. S. ALVES AND C. S. CHEN, A new method of fundamental solutions applied to nonhomogeneous elliptic problems, *Adv. Comput. Math.*, **23**, 125-142, 2005.

[2] J. P. S. AZEVEDO AND L. C. WROBEL, Non-linear heat conduction in composite bodies: A boundary element formulation, *Int. J. Numer. Meth. Eng.*, **26**, 19-38, 1988.

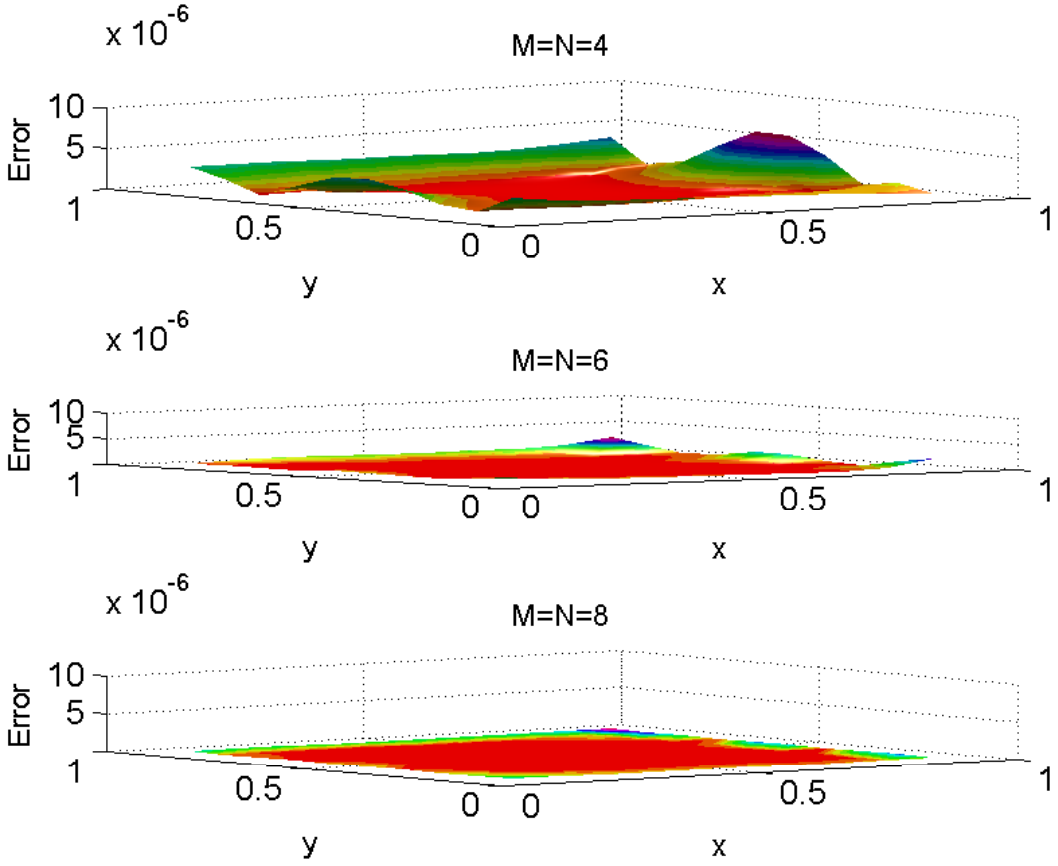

FIGURE 15. Absolute error in temperature at level $z = 0.5$ for various values of $M = N$ in Example 4

[3] J. R. BERGER AND A. KARAGEORGHIS, The method of fundamental solutions for heat conduction in layered materials, *Int. J. Numer. Meth. Eng.*, **45**, 1681-1694, 1999.

[4] J. R. BERGER AND A. KARAGEORGHIS, The method of fundamental solutions for layered elastic materials, *Eng. Anal. Boundary Elements*, **25**, 877-886, 2001.

[5] J. R. BERGER, A. KARAGEORGHIS AND P. A. MARTIN, Stress intensity factor computation using the method of fundamental solutions: Mixed mode problems, *Int. J. Numer. Meth. Eng.*, **69**, 469-483, 2007.

[6] R. BIALECKI AND R. NAHLIK, Solving nonlinear steady-state potential problems in inhomogeneous bodies using the boundary-element method, *Numer. Heat Transfer, Part B*, **16**, 79-96, 1989.

[7] R. BIALECKI AND A. J. NOWAK, Boundary value problems in heat conduction with nonlinear material and nonlinear boundary conditions, *Appl. Math. Modelling*, **5**, 417-421, 1981.

[8] R. BIALECKI AND G. KUHN, Boundary element solution of heat conduction problems in multizone bodies of non-linear material, *Int. J. Numer. Meth. Eng.*, **36**, 799-809, 1993.

[9] A. BOGOMOLNY, Fundamental solutions method for elliptic boundary value problems, *SIAM J. Numer. Anal.*, **22**, 644-669, 1985.

[10] G. BURGESS AND E. MAHAJERIN, A comparison of the boundary element method and superposition methods, *Comput. Structures*, **19**, 697-705, 1984.

[11] H. S. CARSLAW AND J. C. JAEGER, *Conduction of Heat in Solids*, 2nd edn., Clarendon Press, Oxford, 1959.

[12] J. DONEA AND S. GIULIANI, Finite element analysis of steady-state nonlinear heat transfer problems, *Nucl. Eng. Des.*, **30**, 205-213, 1974.

[13] G. FAIRWEATHER, The Method of Fundamental Solutions - A Personal Perspective, Plenary talk at the First International Workshop on the Method of Fundamental Solutions (MFS 2007), Ayia Napa, Cyprus, June 11–13, 2007.

[14] G. FAIRWEATHER AND A. KARAGEORGHIS, The method of fundamental solutions for elliptic boundary value problems, *Adv. Comput. Math.*, **9**, 69-95, 1998.

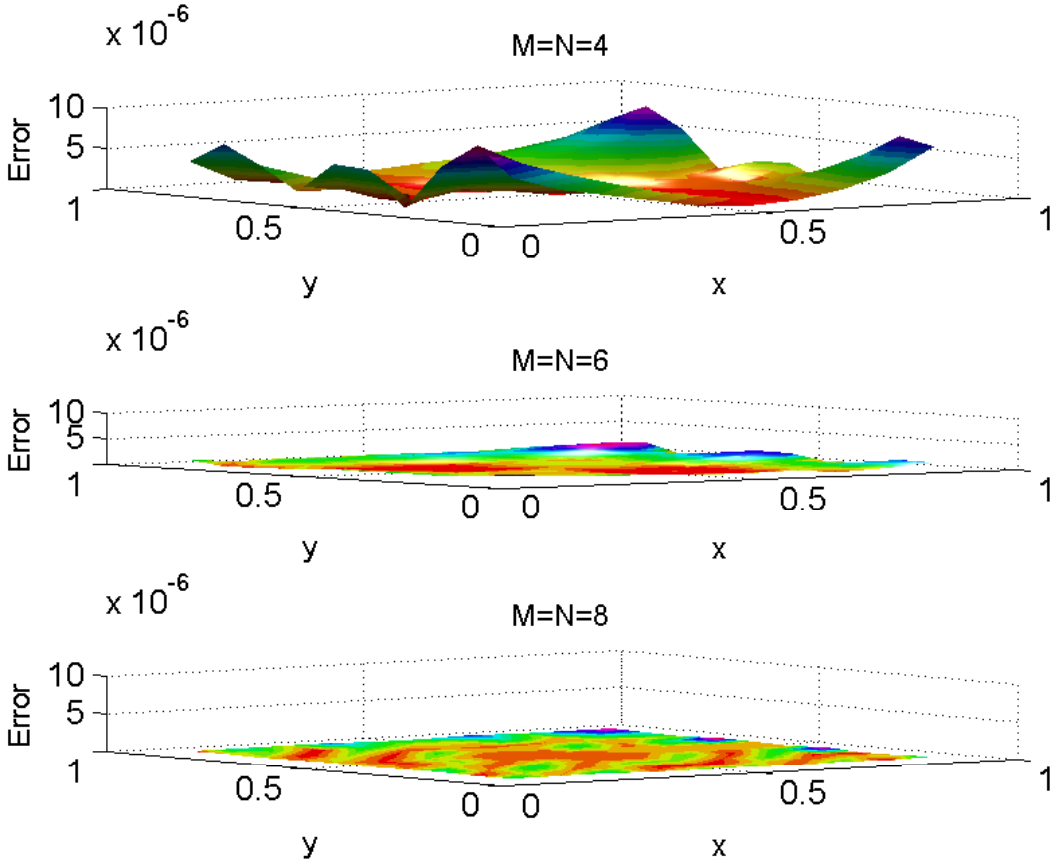

FIGURE 16. Absolute error in temperature at level $z = 0$ for various values of $M = N$ in Example 4

[15] R. T. FENNER, A force superposition approach to plane elastic stress and strain analysis, *J. Strain Anal.*, **36**, 517-529, 2001.

[16] B. S. GARBOW, K. E. HILLSTROM AND J. J. MORÉ, MINPACK Project, Argonne National Laboratory, 1980.

[17] G. N. GATICA AND G. C. HSIAO, *Boundary-Field Equation Methods for a Class of Nonlinear Problems*, Pitman Publishing, London, 1995.

[18] M. A. GOLBERG, The method of fundamental solutions for Poisson's equation, *Eng. Anal. Boundary Elements*, **16**, 205-213, 1995.

[19] M. A. GOLBERG AND C. S. CHEN, The method of fundamental solutions for potential, Helmholtz and diffusion problems, in Boundary Integral Methods: Numerical and Mathematical Aspects, vol. 1 of Comput. Eng., WIT Press/Comput. Mech. Publ., Boston, MA, 1999, pp. 103-176.

[20] D. B. INGHAM, P. J. HEGGS AND M. MANZOOR, Boundary integral equation solution of non-linear plane potential problems, *IMA J. Numer. Anal.*, **1**, 415-426, 1981.

[21] A. KARAGEORGHIS AND G. FAIRWEATHER, The method of fundamental solutions for the solution of the biharmonic equation, *J. Comput. Phys.*, **69**, 434-459, 1987.

[22] A. KARAGEORGHIS AND G. FAIRWEATHER, The method of fundamental solutions for the solution of nonlinear plane potential problems, *IMA J. Numer. Anal.*, **9**, 231-242, 1989.

[23] A. KARAGEORGHIS AND D. LESNIC, The method of fundamental solutions for steady-state heat conduction in nonlinear materials, (submitted).

[24] M. KATSURADA, Asymptotic error analysis of the charge simulation method in a Jordan region with an analytic boundary, *J. Fac. Sci. Univ. Tokyo Sect. 1A Math.*, **37**, 635–657, 1990.

[25] V. M. A. LEITÃO, C. J. S. ALVES AND C. A. DUARTE, *Advances in Meshfree Techniques*, Comput. Meth. Appl. Sci., Vol.5, Springer, Berlin, 2007.

[26] R. MATHON AND R. L. JOHNSTON, The approximate solution of elliptic boundary-value problems by fundamental solutions, *SIAM J. Numer. Anal.*, **14**, 638-650, 1977.

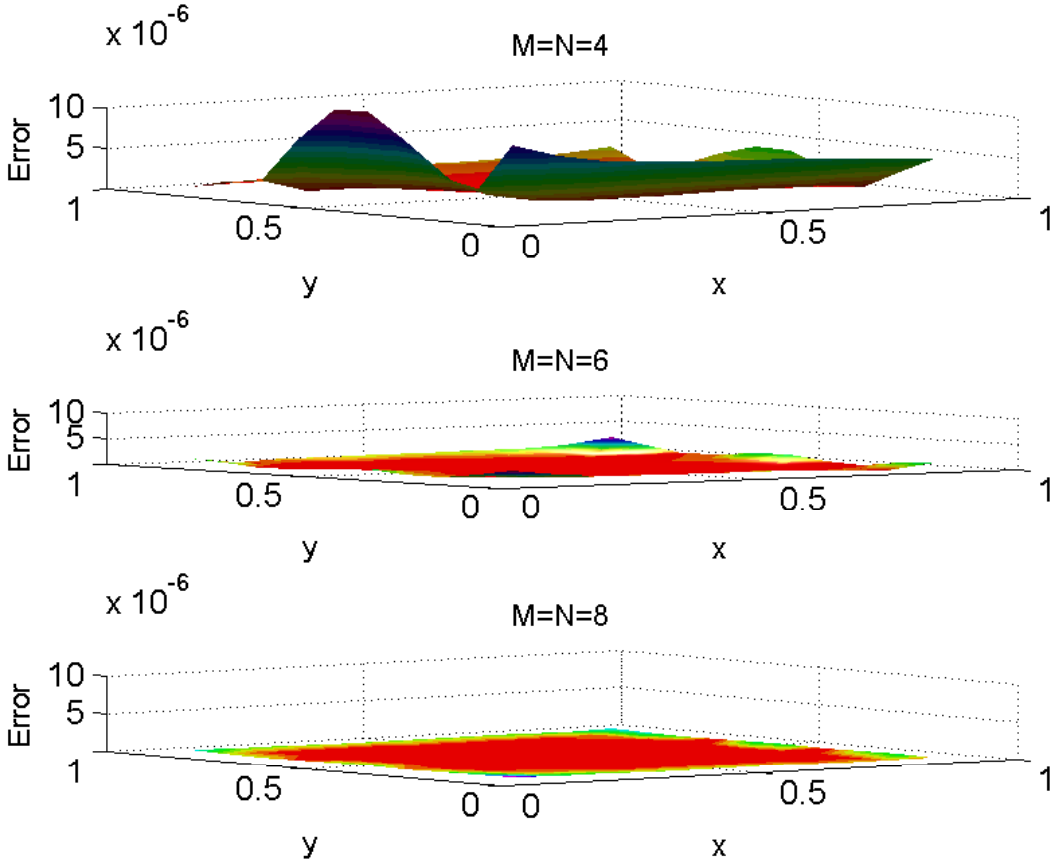

FIGURE 17. Absolute error in temperature at level $z = -0.5$ for various values of $M = N$ in Example 4

[27] M. N. OZISIK, *Boundary Value Problems of Heat Conduction*, International Textbook, Scranton, 1968.

[28] B. SAWAF, M. N. OZISIK AND Y. JARNY, An inverse analysis to estimate linearly dependent thermal conductivity components and heat capacity of an orthotropic medium, *Int. J. Heat Mass Transfer*, **38**, 3005-3010, 1995.

[29] Y-S. SMYRLIS AND A. KARAGEORGHIS, Numerical analysis of the MFS for certain harmonic problems, *M2AN Math. Model. Numer. Anal.*, **38**, 495-517, 2004.

[30] R. TANKELEVICH, G. FAIRWEATHER, A. KARAGEORGHIS AND Y.-S. SMYRLIS, Potential field based geometric modelling using the method of fundamental solutions, *Int. J. Numer. Meth. Eng.*, **68**, 1257-1280, 2006.

[31] Y. S. TOULOUKIAN, *Thermophysical Properties of High Temperature Solid Materials*, McMillan, New York, 1967.

[32] C. C. TSAI, D. L. YOUNG, D. C. LO AND T. K. WONG, Method of fundamental solutions for three-dimensional Stokes flow in exterior field, *J. Eng. Mech.*, **132**, 317–326, 2006.

[33] T. WEI, Y. C. HON AND L. LING, Method of fundamental solutions with regularization techniques for Cauchy problems of elliptic operators, *Eng. Anal. Boundary Elements*, **31**, 373-385, 2007.

DEPARTMENT OF MATHEMATICS AND STATISTICS, UNIVERSITY OF CYPRUS/ ΠΑΝΕΠΙΣΤΗΜΙΟ ΚΥΠΡΟΥ, P.O.BOX 20537, 1678 NICOSIA/ΛΕΥΚΩΣΙΑ, CYPRUS/ΚΥΠΡΟΣ
E-mail address: andreask@ucy.ac.cy

DEPARTMENT OF APPLIED MATHEMATICS, UNIVERSITY OF LEEDS, LEEDS LS2 9JT, UK
E-mail address: amt5ld@maths.leeds.ac.uk